Since January 2020 Elsevier has created a COVID-19 resource centre with free information in English and Mandarin on the novel coronavirus COVID-19. The COVID-19 resource centre is hosted on Elsevier Connect, the company's public news and information website.

Infectious Disease Modelling 7 (2022) 660–689

Contents lists available at ScienceDirect

Infectious Disease Modelling

journal homepage: www.keaipublishing.com/idm

Effect of awareness, quarantine and vaccination as control strategies on COVID-19 with Co-morbidity and Re-infection

Amit Kumar Saha [a, *], Shikha Saha [b], Chandra Nath Podder [a]

[a] Department of Mathematics, University of Dhaka, Dhaka, 1000, Bangladesh
[b] Department of Mathematics, Bangladesh University of Engineering and Technology (BUET), Dhaka, 1000, Bangladesh

ARTICLE INFO

Article history:
Received 8 August 2022
Received in revised form 22 September 2022
Accepted 22 September 2022
Available online 29 September 2022

Keywords:
COVID-19
Co-morbidity
Face-mask
Quarantine
Vaccination
Optimal control
Re-infection

ABSTRACT

In this paper, a deterministic compartmental model is presented to assess the impact of vaccination and non-pharmaceutical interventions (social distance, awareness, face mask, and quarantine) on the transmission dynamics of COVID-19 with co-morbidity and re-infection. An expression for the basic reproduction number is then derived for this model. Theoretical analysis shows that the model exhibits backward bifurcation phenomenon when the basic reproduction number is less than unity. But for the case of no re-infection, the model has a globally asymptotically stable disease-free equilibrium (DFE) when the basic reproduction number is less than unity. Furthermore, it is shown that in the case of no re-infection, a unique endemic equilibrium point (EEP) of the model exists which is globally asymptotically stable whenever the reproduction number is greater than unity. From the global sensitivity and uncertainty analysis, we have identified mask coverage, mask efficacy, vaccine coverage, vaccine efficacy, and contact rate as the most influential parameters influencing the spread of COVID-19. Numerical simulation results show that the use of effective vaccines with proper implementation of non-pharmaceutical interventions could lead to the elimination of COVID-19 from the community. Numerical simulations also suggest that the control strategy that ensures a continuous and effective mass vaccination program is the most cost-effective control strategy. The study also shows that in the presence of any co-morbidity and with the occurrence of re-infection, the disease burden may increase.

1. Introduction

The novel coronavirus (COVID-19) caused by SARS-CoV-2 became a global public health concern in 2020 and 2021 and is still posing a health and economic threat throughout the world (Center for disease control and prevention, coronavirus disease, 2022). Almost all the countries in the world are trying to deal with this new contagious disease and getting rid of it has now become the most important challenge for all countries. It first appeared in China in December 2019 and due to its high infectiousness, it spreads very fast all over the world, putting the world at extreme global crisis (Wu et al., 2020, Bubar et al., 2021). It becomes more dangerous for people of any age with certain medical issues including cardiovascular disease,

* Corresponding author.
E-mail addresses: amit92.du@gmail.com (A.K. Saha), shikhadumath58@gmail.com (S. Saha), cpodder@du.ac.bd (C.N. Podder).
Peer review under responsibility of KeAi Communications Co., Ltd.

https://doi.org/10.1016/j.idm.2022.09.004

diabetes, high blood pressure, cancer, etc (World health organization emergencies preparedness response, 2022). A report from a survey of 138 COVID-19 infected individuals confirms it by showing that more than 45% of the infected individuals had one or more co-morbidities and that infected individuals who were admitted to the intensive care unit (ICU) had a higher number of co-morbidities (72.2%) compared to the infected individuals who didn't admit to the ICU (37.3%) (Jain and Yuan, 2020). As of June 20, 2022, 539928791 people were infected with the Covid-19 and 6320448 people died worldwide (World health organization, 2022).

On the one hand, its high infectious rate, and on the other hand, the frequent emergence of new variants have made the control of COVID-19 even more challenging. In these circumstances, the invention of effective vaccines is not the only way to address this challenge. Hence non-pharmaceutical interventions should also be maintained. At the beginning of 2020, the genetic sequence of SARS-CoV-2 was published. After that, corporations, governments, international health organizations, and university research groups started to work for developing vaccines against COVID-19 (Le et al., 2020, World health organization timeline – covid-19, 2020). After the initial development and three-stage clinical trials for safety and effectiveness, the following vaccines obtained World health organization's EUL (Emergency Use Listing): The Pfizer-BioNTech Comirnaty vaccine on 31 December 2020, the SII/COVIDSHIELD and AstraZeneca/AZD1222 vaccines on 16 February 2021, the Janssen/Ad26.COV 2.S vaccine on 12 March 2021, the Moderna COVID-19 vaccine (mRNA 1273) on 30 April 2021, the Sinopharm COVID-19 vaccine on 7 May 2021, the Sinovac-CoronaVac vaccine on 1 June 2021, the Bharat Biotech BBV152 COVAXIN vaccine on 3 November 2021, the Covovax (NVX-CoV2373) vaccine on 17 December 2021, the Nuvaxovid (NVX-CoV2373) vaccine on 20 December 2021 (World health organization timeline – covid-19, 2022). The Pfizer-BioNTech COVID-19, the Moderna, and the Johnson and Johnson's Janssen vaccines are fully approved by FAD for people 18 years of age and older and only the Pfizer-BioNTech COVID-19 has approbation for emergency use for children ages 5 years and older (Center for disease control and prevention, 2022). More than 529 million vaccine doses have been administered in the United States from 14 December 2020 through 18 January 2022. During this period, the mortality rate received by Vaccine Adverse Event Reporting System (VAERS) was 0.0022% among the people who received a COVID-19 vaccine (Center for disease control and prevention, 2022). Globally a total of 9,571,502,663 vaccine doses have been administered by 18 January 2022 (World health organization, 2022).

Besides the use of effective vaccine and medical research, mathematical models can be a powerful means in getting insight into the dynamics of any infectious disease like COVID-19 which can help decision makers take necessary decisions to prevent the spread of COVID-19. It also helps assess the impact of vaccines and the use of NPIs in controlling the spread of the pandemic and mitigating its life-threatening effects. A significant number of mathematical models have already been developed and used to study the transmission dynamics of COVID-19 and also to control the disease burden. As for example, a mathematical model with fractal-fractional operators has been designed by the authors in Atangana (2020) to assess the effectiveness of lockdown before vaccination. A model for the dynamics of COVID-19 with re-infection has been proposed by the authors in Zamir et al. (2021). The infection dynamics of COVID-19 is studied using mathematical models to assess the impact of NPIs by the authors in Ngonghala et al. (2020). The authors in Gumel et al. (2021) proposed a nonlinear mathematical model to understand the transmission dynamics of COVID-19 in the presece of vaccinations and non-pharmaceutical interventions. A mathematical model with fractional order derivative has been formulated in Khan and Atangana (2020). Impact of co-morbidity, re-infection and NPIs have been investigated by the authors in Saha et al. (2022). Again, to lessen the disease burden, different control measures are implemented in the proposed model (Omame et al., 2020, Das et al., 2021, Shen et al., 2021, Abioye et al., 2021, Asamoah et al., 2022 and so on). Infact, optimal control strategies and cost analysis has become important to suggest effective control strategies to reduce the prevalence of COVID-19 and also to reduce the disease burden. In Omame et al. (2020), using three control strategies authors showed that the most effective one of all the strategies is the one which avoids COVID-19 infection by co-morbid susceptibles. Authors in Das et al. (2021), suggested that a combination of non-pharmaceutical interventions and vaccination can reduce COVID-19 largely. In Shen et al. (2021), using four control strategies authors showed that considering effective control strategies, infected cases can be reduced. In the work Abioye et al. (2021), three control strategies are considered and it was shown that multifaceted approach is required to fight against COVID-19. Bandekar and Ghosh (2022), also performed optimal control analysis. Their analysis reveals that if policies related to testing, contact tracing, and mask-wearing are implemented, the spread of COVID-19 can be reduced. In Asamoah et al. (2022), authors implemented four control strategies considering all possible combinations of the strategies and they showed that practicing physical or social distancing protocols is the most cost-effective strategy. There are many other interesting articles related to COVID-19, some of which can be mentioned here (Ivorra et al., 2020, Kucharski et al., 2020, Mizumoto and Chowell, 2020, Ferguson et al., 2020, p. 20, Okuonghae and Omame, 2020, Mancuso et al., 2021, Srivastav et al., 2021) and the references therein.

Motivated by the above investigations on COVID-19, we have formulated a new mathematical model for the transmission dynamics of COVID-19 based on the model (Saha et al., 2022) incorporating vaccination of the susceptible individuals and also considering re-infection of the recovered individuals. We have also considered vaccinating a portion of the recovered individuals who have yet to be immunized. The aim of this research is to assess the impact of vaccination and non-pharmaceutical interventions (NPIs) on the spread of COVID-19. Our aim is also to highlight the effect of co-morbidity and re-infection on the transmission dynamics of COVID-19. In this paper, we have also implemented four control strategies considering all possible combinations of the strategies during the numerical simulation of the optimal control problem which is a new feature of this paper as the control strategies are different from Asamoah et al. (2022) and Shen et al. (2021). The

sensitivity analysis of the parameter of our model with respect to some response functions is performed to detect which parameters have greater impact on the transmission of COVID-19.

The entire paper is decorated in the following manners. In section 2, the formulation of the COVID-19 model is presented and non-negativity and boundedness of the model solutions are proved. Section 3 is engaged with the rigorous theoretical analysis of the model to discuss about the stability of equilibrium. In section 5, the model is extended based on optimal control theory and analyzed mathematically to prove the existence of an optimal control using the Pontryagin's maximum principle. Numerical simulations are presented in section 6. Section 7 is devoted to the discussion and conclusion about the findings.

2. Model formulation

We develop the model by dividing the total human population at time t, denoted by $N(t)$, into twelve mutually exclusive classes: susceptible ($S(t)$), susceptible with co-morbidity ($S_c(t)$), vaccinated ($S_v(t)$), exposed in early stage ($E_1(t)$), pre-symptomatic ($E_2(t)$), asymptomatic infected without co-morbidity ($I_a(t)$), symptomatic infected without co-morbidity ($I_s(t)$), asymptomatic infected with co-morbidity ($I_{ac}(t)$), symptomatic infected with co-morbidity ($I_{sc}(t)$), quarantined ($Q(t)$), hospitalized ($H(t)$) and recovered ($R(t)$), so that.

$$N(t) = S(t) + S_c(t) + S_v(t) + E_1(t) + E_2(t) + I_a(t) + I_s(t) + I_{ac}(t) + I_{sc}(t) + Q(t) + H(t) + R(t).$$

To formulate the model we consider the following assumptions:

- Birth rate is not considered.
- Exposed individuals in early stage are asymptotically infected and unable to infect others.
- Pre-symptomatic infectious individuals are shedding viruses and can infect others.
- Quarantine and hospitalization are perfect and individuals belonging to these classes can not infect others.
- Individuals recovered from COVID-19 may again return to exposed in early stage class at a lower rate.

Susceptible individuals acquire infection with COVID-19 upon contacting with individuals in the E_2, I_a, I_s, I_{ac} and I_{sc} classes, at a rate λ, where

$$\lambda = \frac{(1 - e\,m)\,\beta\,(\eta_e E_2 + \eta_a I_a + I_s + \mathscr{T}_1 I_{ac} + \mathscr{T}_2 I_{sc})}{N - (Q + H)}, \tag{1}$$

where, β represents the contact rate for effective transmission of COVID-19. $0 < m \leq 1$ represents the percentage of mask coverage and $0 < e \leq 1$ indicates face masks efficacy. It is assumed that pre-symptomatic individuals (E_2 class) and asymptomatic infected individuals (I_a class) infect others at a lower rate, $\eta_e\,\beta$ and $\eta_a\,\beta$, respectively with $0 < \eta_e, \eta_a < 1$. Furthermore modification parameter $\mathscr{T}_1, \mathscr{T}_2 > 1$ indicate individuals in I_{ac} and I_{sc} classes can transmit COVID-19 at an increased rate, $\mathscr{T}_1\,\beta$ and $\mathscr{T}_2\,\beta$, respectively.

The equations for the transmission dynamics of COVID-19 with co-morbidity in the presence of vaccination is given by the following system of non-linear differential equations (the schematic diagram of the model is shown in Fig. 1 and the parameters are described in details in Table 1).

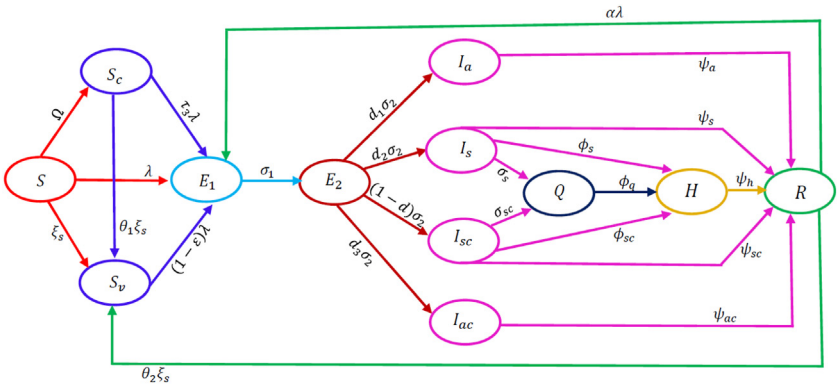

Fig. 1. Schematic diagram of the COVID-19 model (2).

Table 1
Model parameters with description.

Parameter	Description
Λ	Recruitment rate
β	Effective contact rate for COVID-19 transmission
ξ_s	Vaccination rate for susceptible individuals
ϵ	Vaccine efficacy
m	Proportion of individuals who use masks
e	Face mask efficacy
$\mathscr{T}_1, \mathscr{T}_2$	Relative risk of high infectiousness of individuals in I_{ac} and I_{sc} classes compared to individuals in I_s class
$\mathscr{T}_3$	Modification parameter accounting for increased susceptibility to COVID-19 infection by co-morbid susceptible
η_e, η_a	Relative risk of low infectiousness of individuals in E_1 and I_a classes compared to individuals in I_s class
Ω	Proportion of co-morbid susceptible individuals
α	Re-infection rate of recovered individuals
σ_1	Progression rate of early exposed individuals (E_1) to pre-symptomatic (E_2) class
σ_2	Rate of progression of pre-symptomatic (E_2) individuals to infectious classes (I_a, I_s, I_{ac} and I_{sc}, respectively)
d_1, d_2 and d_3	Fraction of pre-symptomatic individuals who progress to the I_a, I_s and I_{ac} classes, respectively ($d_1 + d_2 + d_3 \leq 1$)
$1 - (d_1 + d_2 + d_3)$	Fraction of individuals move from E_2 class to I_{sc} class
σ_s and σ_{sc}	Transmission rate from I_s and I_{sc} classes to Q class, respectively
φ_s, φ_{sc} and φ_q	Transition rate from I_s, I_{sc} and Q classes to H class, respectively
ψ_a, ψ_s, ψ_{ac}, ψ_{sc}, ψ_q and ψ_h	Recovery rate of individuals from I_a, I_s, I_{ac}, I_{sc}, Q and H classes, respectively
δ_e, δ_a, δ_s, δ_{ac}, δ_{sc} and δ_h	Disease related death rate for individuals in the E_2, I_a, I_s, I_{ac}, I_{sc} and H classes, respectively
μ	Natural death rate
θ_1	modification parameter ($\theta_1 > 1$) implying high vaccination rate provided to the co-morbid susceptible individuals
θ_2	modification parameter ($0 < \theta_2 < 1$) implying low vaccination rate provided to the recovered individuals

$$
\begin{aligned}
\dot{S} &= \Lambda - \lambda S - (\Omega + \xi_s + \mu)S,\\
\dot{S}_c &= \Omega S - \mathscr{T}_3 \lambda S_c - (\theta_1 \xi_s + \mu) S_c,\\
\dot{S}_v &= \xi_s S + \theta_1 \xi_s S_c + \theta_2 \xi_s R - (1-\epsilon)\lambda S_v - \mu S_v,\\
\dot{E}_1 &= \lambda S + \mathscr{T}_3 \lambda S_c + (1-\epsilon)\lambda S_v + \alpha \lambda R - (\sigma_1 + \mu) E_1,\\
\dot{E}_2 &= \sigma_1 E_1 - (\sigma_2 + \delta_e + \mu) E_2,\\
\dot{I}_a &= d_1 \sigma_2 E_2 - (\psi_a + \delta_a + \mu) I_a,\\
\dot{I}_s &= d_2 \sigma_2 E_2 - (\sigma_s + \psi_s + \varphi_s + \delta_s + \mu) I_s,\\
\dot{I}_{ac} &= d_3 \sigma_2 E_2 - (\psi_{ac} + \delta_{ac} + \mu) I_{ac},\\
\dot{I}_{sc} &= (1-d)\sigma_2 E_2 - (\sigma_{sc} + \psi_{sc} + \varphi_{sc} + \delta_{sc} + \mu) I_{sc},\\
\dot{Q} &= \sigma_s I_s + \sigma_{sc} I_{sc} - (\psi_q + \varphi_q + \mu) Q,\\
\dot{H} &= \varphi_s I_s + \varphi_{sc} I_{sc} + \varphi_q Q - (\psi_h + \delta_h + \mu) H,\\
\dot{R} &= \psi_a I_a + \psi_s I_s + \psi_{ac} I_{ac} + \psi_{sc} I_{sc} + \psi_q Q + \psi_h H - \alpha \lambda R - (\theta_2 \xi_s + \mu) R,
\end{aligned}
\tag{2}
$$

where, $d = d_1 + d_2 + d_3$.

Λ is the recruitment rate of susceptible humans into the population. Ω represents the ratio of susceptible individuals who have co-morbidity. It is assumed that susceptible individuals having co-morbidity are more susceptible to COVID-19 infection ($\mathscr{T}_3\ \lambda$ with $\mathscr{T}_3 > 1$) than susceptible individuals having no co-morbidity.

3. Theoretical analysis

3.1. Fundamental properties

3.1.1. Non-negativity of the solutions

To show the non-negativity of the solutions we prove the following theorem.

Theorem 1. *The solutions of the model* (2)*, with initial conditions* $S(0) > 0, S_c(0) \geq 0, S_v(0) \geq 0, E_1(0) \geq 0, E_2(0) \geq 0, I_a(0) \geq 0, I_s(0) \geq 0, I_{ac}(0) \geq 0, I_{sc}(0) \geq 0, Q(0) \geq 0, H(0) \geq 0$, and $R(0) \geq 0$ *are positive for all time* $t > 0$.

Proof. Let $\{S, S_c, S_v, E_1, E_2, I_a, I_s, I_{ac}, I_{sc}, Q, H, R\}$ be the set of solutions of the model (2). From the first equation of the model (2) we can write

$$\frac{d}{dt}\left[S(t)\exp\left\{\int_0^t \lambda(u)\,du + k_1\,t\right\}\right] = \Lambda\left[\exp\left\{\int_0^t \lambda(u)\,du + k_1\,t\right\}\right], \tag{3}$$

where, $k_1 = \Omega + \xi_s + \mu$.

From (3),

$$S(t)\exp\left\{\int_0^t \lambda(u)\,du + k_1\,t\right\} - S(0) = \int_0^t \Lambda\left[\exp\left\{\int_0^x \lambda(u)\,du + k_1\,t\right\}\right]dx.$$

Hence,

$$S(t) = S(0)\exp\left\{-\int_0^t \lambda(u)\,du + k_1\,t\right\} + \exp\left\{-\int_0^t \lambda(u)\,du + k_1\,t\right\}\int_0^t \Lambda\left[\exp\left\{\int_0^x \lambda(u)\,du + k_1\,t\right\}\right]dx > 0.$$

Proceeding in the same way, it can be shown that.

$S_c \geq 0$, $S_v \geq 0$, $E_1 \geq 0$, $E_2 \geq 0$, $I_a \geq 0$, $I_s \geq 0$, $I_{ac} \geq 0$, $I_{sc} \geq 0$, $Q \geq 0$, $H \geq 0$, and $R \geq 0$ for all $t \geq 0$. □

3.1.2. Boundedness of the solution

Adding all the equations of the model (2), we get

$$\frac{dN}{dt} = \Lambda - \mu N - \delta_e E_2 - \delta_a I_a - \delta_s I_s - \delta_{ac} I_{ac} - \delta_{sc} I_{sc} - \delta_h H. \tag{4}$$

It is obvious that $0 < E_2 \leq N$, $0 < I_a \leq N$, $0 < I_s \leq N$, $0 < I_{ac} \leq N$, $0 < I_{sc} \leq N$, $0 < H \leq N$.

It follows that

$$\Lambda - (\mu + \delta_e + \delta_a + \delta_s + \delta_{ac} + \delta_{sc} + \delta_h)\,N \leq \frac{dN}{dt} < \Lambda - \mu N, \tag{5}$$

Thus, $\frac{\Lambda}{\mu+\delta_e+\delta_a+\delta_s+\delta_{ac}+\delta_{sc}+\delta_h} \leq \liminf_{t\to\infty} N \leq \limsup_{t\to\infty} N \leq \frac{\Lambda}{\mu}$.

This implies $\limsup_{t\to\infty} N \leq \frac{\Lambda}{\mu}$.

3.1.3. Invariant regions

Now let us consider the region $\mathscr{D} = \left\{(S, S_c, S_v, E_1, E_2, I_a, I_s, I_{ac}, I_{sc}, Q, H, R) \in \mathbb{R}_+^{12} : N \leq \frac{\Lambda}{\mu}\right\}$.

From equations (4) and (5) we can write

$$\frac{dN}{dt} \leq \Lambda - \mu N. \tag{6}$$

Solving this and using a comparison theorem as described in Lakshmikantham et al. (1989) we have $N(t) \leq N(0)\,e^{-\mu t} + \frac{\Lambda}{\mu}\,(1 - e^{-\mu t})$. Particularly, it can be shown that $N(t) \leq \frac{\Lambda}{\mu}$ if $N(0) \leq \frac{\Lambda}{\mu}$. This implies all the solutions of system (2) with initial conditions in $\mathscr{D}$ remains in $\mathscr{D}$ for all time $t > 0$. Thus, the region $\mathscr{D}$ is positive invariant and attracting (Hethcote, 2000).

3.2. Local asymptotic stability of the DFE

From the COVID-19 model (2), the disease-free equilibrium, $\mathscr{E}_0$, is obtained as

$$\mathscr{E}_0 = (S^*, S_c^*, S_v^*, E_1^*, E_2^*, I_a^*, I_s^*, I_{ac}^*, I_{sc}^*, Q^*, H^*, R^*) = \left(\frac{\Lambda}{k_1}, \frac{\Omega\,\Lambda}{k_1\,k_2}, \frac{\Lambda\,\xi_s\,(k_2 + \Omega\,\theta_1)}{k_1\,k_2\,k_3}\ 0, 0, 0, 0, 0, 0, 0, 0, 0\right). \tag{7}$$

To establish the condition for local asymptotic stability (LAS) of the DFE, the next generation operator method described in Diekmann et al. (1990), Van den Driessche and Watmough (2002) is used. The next generation matrices for the new infection terms and remaining transfer terms, denoted by F and V respectively, are given by

$$F = \begin{pmatrix} 0 & F_e & F_a & F_s & F_{ac} & F_{sc} & 0 & 0 \\ 0 & 0 & 0 & 0 & 0 & 0 & 0 & 0 \\ 0 & 0 & 0 & 0 & 0 & 0 & 0 & 0 \\ 0 & 0 & 0 & 0 & 0 & 0 & 0 & 0 \\ 0 & 0 & 0 & 0 & 0 & 0 & 0 & 0 \\ 0 & 0 & 0 & 0 & 0 & 0 & 0 & 0 \\ 0 & 0 & 0 & 0 & 0 & 0 & 0 & 0 \end{pmatrix}, V = \begin{pmatrix} k_4 & 0 & 0 & 0 & 0 & 0 & 0 & 0 \\ -\sigma_1 & k_5 & 0 & 0 & 0 & 0 & 0 & 0 \\ 0 & -d_1\,\sigma_2 & k_6 & 0 & 0 & 0 & 0 & 0 \\ 0 & -d_2\,\sigma_2 & 0 & k_7 & 0 & 0 & 0 & 0 \\ 0 & -d_3\,\sigma_2 & 0 & 0 & k_8 & 0 & 0 & 0 \\ 0 & -(1-d)\,\sigma_2 & 0 & 0 & 0 & k_9 & 0 & 0 \\ 0 & 0 & 0 & -\sigma_s & 0 & -\sigma_{sc} & k_{10} & 0 \\ 0 & 0 & 0 & -\varphi_s & 0 & -\varphi_{sc} & 0 & k_{11} \end{pmatrix},$$

where.

$F_e = (1-em)\,\beta\,\eta_e \frac{S^*+\tau_3\,S_c^*+(1-\epsilon)\,S_v^*+\alpha\,R^*}{N^{**}}$, $F_a = (1-em)\,\beta\,\eta_a \frac{S^*+\tau_3\,S_c^*+(1-\epsilon)\,S_v^*+\alpha\,R^*}{N^{**}}$, $F_s = (1-em)\,\beta\,\frac{S^*+\tau_3\,S_c^*+(1-\epsilon)\,S_v^*+\alpha\,R^*}{N^{**}}$,

$F_{ac} = (1-em)\,\beta\,\tau_1 \frac{S^*+\tau_3\,S_c^*+(1-\epsilon)\,S_v^*+\alpha\,R^*}{N^{**}}$, $F_{sc} = (1-em)\,\beta\,\tau_2 \frac{S^*+\tau_3\,S_c^*+(1-\epsilon)\,S_v^*+\alpha\,R^*}{N^{**}}$, $N^{**} = N^* - (Q^*+H^*)$,

$k_1 = \Omega+\xi_s+\mu$, $k_2 = \theta_1\,\xi_s+\mu$, $k_3 = \mu$, $k_4 = \sigma_1+\mu$, $k_5 = \sigma_2+\delta_e+\mu$, $k_6 = \psi_a+\delta_a+\mu$, $k_7 = \sigma_s+\psi_s+\varphi_s+\delta_s+\mu$,

$k_8 = \psi_{ac}+\delta_{ac}+\mu, k_9 = \sigma_{sc}+\psi_{sc}+\varphi_{sc}+\delta_{sc}+\mu$, $k_{10} = \psi_q+\varphi_q+\mu$, $k_{11} = \psi_h+\delta_h+\mu$, $k_{12} = \theta_2\,\xi_s+\mu$ and $d = d_1+d_2+d_3$

.

Following the approach described in Chavez et al. (2002), Hethcote (2000), it can be shown that the basic reproduction number, denoted by $\mathscr{R}_c$, is given by

$$\mathscr{R}_c = \rho\,(F\,V^{-1}) = \mathscr{R}_e+\mathscr{R}_a+\mathscr{R}_s+\mathscr{R}_{ac}+\mathscr{R}_{sc}, \tag{8}$$

where, ρ represents the spectral radius of the next generation matrix $F\,V^{-1}$ and

$$\mathscr{R}_e = F_e\,B_e,\ \mathscr{R}_a = F_a\,B_a,\ \mathscr{R}_s = F_s\,B_s,\ \mathscr{R}_{ac} = F_{ac}\,B_{ac},\ \mathscr{R}_{sc} = F_{sc}\,B_{sc},$$

with,

$$B_e = \frac{\sigma_1}{k_4\,k_5},\ B_a = \frac{\sigma_1\,\sigma_2\,d_1}{k_4\,k_5\,k_6},\ B_s = \frac{\sigma_1\,\sigma_2\,d_2}{k_4\,k_5\,k_7},\ B_{ac} = \frac{\sigma_1\,\sigma_2\,d_3}{k_4\,k_5\,k_8},\ B_{sc} = \frac{\sigma_1\,\sigma_2\,(1-d)}{k_4\,k_5\,k_9}.$$

Consequently, using Theorem 2 of Van den Driessche and Watmough (2002) the following result can be established.

Lemma 1. *The DFE of the COVID-19 model given by* (2)*, is locally-asymptotically stable (LAS) if* $\mathscr{R}_c < 1$*, and unstable if* $\mathscr{R}_c > 1$.

3.3. Endemic equilibrium point (EEP)

Let $\mathscr{E}_1 = (S^*, S_c^*, S_v^*, E_1^*, E_2^*, I_a^*, I_s^*, I_{ac}^*, I_{sc}^*, Q^*, H^*, R^*)$ be any equilibrium point of the model (2) and let

$$\lambda^* = \frac{\beta\,(1-em)\,(\eta_e\,E_2^*+\eta_a\,I_a^*+I_s^*+\tau_1\,I_{ac}^*+\tau_2\,I_{sc}^*)}{N^*-(Q^*+H^*)} \tag{9}$$

Now setting the left hand side of each equation of system (2) to zero and solving for the variables we have,

$$
\begin{aligned}
S_c^* &= \frac{\Omega S^*}{(\tau_3 \lambda^* + k_2)},\\
S_v^* &= \frac{A_7 \lambda^{*3} + A_8 \lambda^{*2} + A_9 \lambda^* + A_{10}}{\{(1-\epsilon)\lambda^* + k_3\}(\tau_3 \lambda^* + k_2)(A_4 \lambda^{*2} + A_5 \lambda^* + A_6)} S^*,\\
E_1^* &= \lambda \frac{(A_1 \lambda^{*2} + A_2 \lambda^* + A_3)(\alpha\lambda + k_{12})}{(A_4 \lambda^{*2} + A_5 \lambda^* + A_6)(\tau_3 \lambda^* + k_2)} S^*,\\
E_2^* &= W_e E_1^*,\ I_a^* = W_a E_1^*,\ I_s^* = W_s E_1^*,\ I_{ac}^* = W_{ac} E_1^*,\ I_{sc}^* = W_{sc} E_1^*,\ Q^* = W_q E_1^*,\ H^* = W_h E_1^*,\\
R^* &= \frac{W_r}{\alpha \lambda^* + k_{12}} E_1^*,
\end{aligned}
\tag{10}
$$

where.

$$
\begin{aligned}
&W_e = \frac{\sigma_1}{k_5},\ W_a = \frac{d_1 \sigma_1 \sigma_2}{k_5 k_6},\ W_s = \frac{d_2 \sigma_1 \sigma_2}{k_5 k_7},\ W_{ac} = \frac{d_3 \sigma_1 \sigma_2}{k_5 k_8},\ W_{sc} = \frac{(1-d)\sigma_1\sigma_2}{k_5 k_9},\ W_q = \frac{(\sigma_s W_s + \sigma_{sc} W_{sc})}{k_{10}},\\
&W_h = \frac{\varphi_s W_s + \varphi_{sc} W_{sc} + \varphi_q W_q}{k_{11}},\ W_r = \psi_a W_a + \psi_s W_s + \psi_{ac} W_{ac} + \psi_{sc} W_{sc} + \psi_q W_q + \psi_h W_h,\\
&A_1 = (1-\epsilon)\tau_3,\ A_2 = (1-\epsilon)k_2 + (1-\epsilon)\tau_3\Omega + \{k_3 + (1-\epsilon)\xi_s\}\tau_3,\ A_3 = \{k_3 + (1-\epsilon)\xi_s\}k_2 + \{k_3\tau_3 + (1-\epsilon)\theta_1\xi_s\}\Omega,\\
&A_4 = \alpha(1-\epsilon)k_4 - (1-\epsilon)\alpha W_r,\ A_5 = (1-\epsilon)k_4 k_{12} + k_4 k_3 \alpha - \{\alpha k_3 + (1-\epsilon)\theta_2\xi_s\}W_r,\ A_6 = k_3 k_4 k_{12},\ A_7 = A_4\tau_3\xi_s,\\
&A_8 = \xi_s(\tau_3 A_5 + A_4 k_2) + A_4\Omega\theta_1\xi_s + A_1\theta_2\xi_s W_r,\ A_9 = \xi_s(\tau_3 A_6 + A_5 k_2) + A_5\Omega\theta_1\xi_s + A_2\theta_2\xi_s W_r,\\
&A_{10} = A_6\Omega\theta_1\xi_s + A_3\theta_2\xi_s B_r.
\end{aligned}
$$

Substituting (10) into (9) gives

$$
\lambda^* = \frac{\beta(1-em)(\eta_e W_e + \eta_a W_a + W_s + \tau_1 W_{ac} + \tau_2 W_{sc})E_1^*}{S^* + \frac{\Omega}{(\tau_3\lambda^* + k_2)}S^* + \frac{A_7\lambda^{*3} + A_8\lambda^{*2} + A_9\lambda^* + A_{10}}{\{(1-\epsilon)\lambda^* + k_3\}(\tau_3\lambda^* + k_2)(A_4\lambda^{*2} + A_5\lambda^* + A_6)}S^* + \left(W_c + \frac{W_r}{\alpha\lambda^* + K_{11}}\right)E_1^*},
\tag{11}
$$

where.

$W_c = 1 + W_e + W_a + W_s + W_{ac} + W_{sc}$.

After some algebraic calculation we get the following equation in terms of λ^*

$$
\lambda^*\left\{P_5\lambda^{*5} + P_4\lambda^{*4} + P_3\lambda^{*3} + P_2\lambda^{*2} + P_1\lambda^* + P_0\right\} = 0,
\tag{12}
$$

where.

$$
\begin{aligned}
P_5 &= W_c\alpha(1-\epsilon)A_1,\\
P_4 &= A_1 W_c\alpha k_3 + (1-\epsilon)A_1(W_c k_{12} + W_r) + A_2 W_c\alpha(1-\epsilon) + A_4\tau_3(1-\epsilon) - A_1(1-\epsilon)\alpha,\\
P_3 &= A_4\tau_3 k_3 + (1-\epsilon)A_4 k_2 + (1-\epsilon)A_5\tau_3 + A_7 + A_1 k_3(W_c k_{12} + W_r) + A_2 W_c\alpha k_3 + (1-\epsilon)A_2(W_c k_{12} + W_r) +\\
&\quad A_3 W_c\alpha(1-\epsilon) - A_1(1-\epsilon)k_{12} - A_1\alpha k_3 - A_2(1-\epsilon)\alpha,\\
P_2 &= A_4 k_2 k_3 + A_6\tau_3(1-\epsilon) + A_5\tau_3 k_3 + A_5(1-\epsilon)k_2 + A_8 + A_3 W_c\alpha k_3 + (1-\epsilon)A_3(W_c k_{12} + W_r) +\\
&\quad A_2 k_3(B_c k_{12} + W_r) - A_1 k_3 k_{12} + A_3(1-\epsilon)\alpha + A_2(1-\epsilon)k_{12} + A_2\alpha k_3,\\
P_1 &= A_5 k_2 k_3 + A_6\tau_3 k_3 + (1-\epsilon)k_2 A_6 + A_9 + A_3 k_3 W_c k_{12} + A_3 k_3 W_r - A_2 k_3 k_{12} - A_3(1-\epsilon)k_{12} - A_3\alpha k_3,\\
P_0 &= A_6 k_2 k_3 + A_{10} - A_3 k_3 k_{12}.
\end{aligned}
$$

Out of the six roots, the root $\lambda^* = 0$, of (12), corresponds to the DFE $\mathscr{E}_0$. Equation (12) says that the non-zero equilibria of the model satisfy

$$f(\lambda^*) = P_5\,\lambda^{*5} + P_4\,\lambda^{*4} + P_3\,\lambda^{*3} + P_2\,\lambda^{*2} + P_1\,\lambda^* + P_0 = 0. \tag{13}$$

Using the parameter values as given in Table 2, it can be shown that $\mathscr{R}_c < 1$ and out of the five roots, two roots are real positive, one is real negative and other two roots are complex. Thus there exists two positive endemic equilibria of system (2) which implies the possibility of the presence of backward bifurcation phenomena.

3.4. Backward bifurcation analysis

Here we will discuss about the possibility of having backward bifurcation phenomena. To explore this phenomena we will use the center manifold theory described in Carr (2012), Van den Driessche and Watmough (2002) and apply change of variable formula. For this, let $S = x_1$, $S_c = x_2$, $S_v = x_3$, $E_1 = x_4$, $E_2 = x_5$, $I_a = x_6$, $I_s = x_7$, $I_{ac} = x_8$, $I_{sc} = x_9$, $Q = x_{10}$, $H = x_{11}$ and $R = x_{12}$, and hence model (2) can be written as $\frac{dX}{dt} = (f_1, f_2, f_3, f_4, f_5, f_6, f_7, f_8, f_9, f_{10}, f_{11}, f_{12})^T$, where $X = (x_1, x_2, x_3, x_4, x_5, x_6, x_7, x_8, x_9, x_{10}, x_{11}, x_{12})^T$ and then we have

$$\begin{aligned}
\frac{dx_1}{dt} &= f_1 = \Lambda - \lambda x_1 - k_1 x_1,\\
\frac{dx_2}{dt} &= f_2 = \Omega x_1 - \mathscr{T}_3\,\lambda x_2 - k_2 x_2,\\
\frac{dx_3}{dt} &= f_3 = \xi_s x_1 + \theta_1 \xi_s x_2 + \theta_2 \xi_s x_{12} - (1-\epsilon)\lambda x_3 - k_3 x_3,\\
\frac{dx_4}{dt} &= f_4 = \lambda x_1 + \mathscr{T}_3\,\lambda x_2 + (1-\epsilon)\lambda x_3 + \alpha\lambda x_{12} - k_4 x_4,\\
\frac{dx_5}{dt} &= f_5 = \sigma_1 x_4 - k_5 x_5,\\
\frac{dx_6}{dt} &= f_6 = d_1\sigma_2 x_5 - k_6 x_6,\\
\frac{dx_7}{dt} &= f_7 = d_2\sigma_2 x_5 - k_7 x_7,\\
\frac{dx_8}{dt} &= f_8 = d_3\sigma_2 x_5 - k_8 x_8,\\
\frac{dx_9}{dt} &= f_9 = (1-d)\sigma_2 x_5 - k_9 x_9,\\
\frac{dx_{10}}{dt} &= f_{10} = \sigma_s x_7 + \sigma_{sc} x_9 - k_{10} x_{10},\\
\frac{dx_{11}}{dt} &= f_{11} = \varphi_s x_7 + \varphi_{sc} x_9 + \varphi_q x_{10} - k_{11} x_{11},\\
\frac{dx_{12}}{dt} &= f_{12} = \psi_a x_6 + \psi_s x_7 + \psi_{ac} x_8 + \psi_{sc} x_9 + \psi_q x_{10} + \psi_h x_{11} - \alpha\lambda x_{12} - k_{12} x_{12},
\end{aligned} \tag{14}$$

$$\lambda = \frac{(1-e\,m)\,\beta\,(\eta_e x_5 + \eta_a x_6 + x_7 + \mathscr{T}_1 x_8 + \mathscr{T}_2 x_9)}{N - (x_{10} + x_{11})}.$$

The Jacobian of system (14) is given by:

Table 2
Estimated parameters for model (2).

Parameter	Baseline Values	Units	References
Λ	5000	Day^{-1}	Estimated from Omame et al. (2020)
β	0.395	Day^{-1}	Fitted
m	0.4	-	Ngonghala et al. (2020)
e	0.8	-	Ngonghala et al. (2020)
$\mathscr{T}_1, \mathscr{T}_2$	1.15, 1.25	-	Fitted
$\mathscr{T}_3$	1.5	-	Fitteed
η_e, η_a	0.6, 0.65	-	Fitted
ξ_s	0.0001	Day^{-1}	Fitted
α	0.0001	Day^{-1}	Estimated from Omame et al. (2020)
ϵ	0.001	-	Estimated from Omame et al. (2020)
σ_1, σ_2	0.2, 0.11	Day^{-1}	Ngonghala et al. (2020)
d_1, d_2 and d_3	0.25, 0.525, 0.075	-	Assumed
$1-(d_1+d_2+d_3)$	0.15	-	Assumed
σ_s, σ_{sc}	0.116, 0.2	Day^{-1}	Ngonghala et al. (2020)
Ω	0.2	Day^{-1}	Ngonghala et al. (2020)
φ_s, φ_{sc} and φ_q	0.15, 0.2, 0.25	Day^{-1}	Fitted
ψ_a, ψ_s, ψ_{ac}, ψ_{sc}, ψ_q and ψ_h	0.14, 0.12, 0.13, 0.11, 0.2, 0.09	Day^{-1}	Ngonghala et al. (2020)
δ_e, δ_a, δ_s, δ_{ac}, δ_{sc} and δ_h	0.0095, 0.02, 0.025, 0.03, 0.0095, 0.015	Day^{-1}	Ngonghala et al. (2020)
μ	0.0001	Day^{-1}	Ngonghala et al. (2020)
θ_1, θ_2	1.2, 0.8	-	Fitted

$$J(\mathscr{E}_0)=\begin{pmatrix}
-k_1 & 0 & 0 & 0 & -\eta_e J_1 & -\eta_a J_1 & -J_1 & -\tau_1 J_1 & -\tau_2 J_1 & 0 & 0 & 0\\
\Omega & -k_2 & 0 & 0 & -\eta_e J_2 & -\eta_a J_2 & -J_2 & -\tau_1 J_2 & -\tau_2 J_2 & 0 & 0 & 0\\
\xi_s & \theta_1\xi_s & -k_3 & 0 & -\eta_e J_3 & -\eta_a J_3 & -J_3 & -\tau_1 J_3 & -\tau_2 J_3 & 0 & 0 & \theta_2\xi_s\\
0 & 0 & 0 & -k_4 & \eta_e J_4 & \eta_a J_4 & J_4 & \tau_1 J_4 & \tau_2 J_4 & 0 & 0 & 0\\
0 & 0 & 0 & \sigma_1 & -k_5 & 0 & 0 & 0 & 0 & 0 & 0 & 0\\
0 & 0 & 0 & 0 & d_1\sigma_2 & -k_6 & 0 & 0 & 0 & 0 & 0 & 0\\
0 & 0 & 0 & 0 & d_2\sigma_2 & 0 & -k_7 & 0 & 0 & 0 & 0 & 0\\
0 & 0 & 0 & 0 & d_3\sigma_2 & 0 & 0 & -k_8 & 0 & 0 & 0 & 0\\
0 & 0 & 0 & 0 & (1-d)\sigma_2 & 0 & 0 & 0 & -k_9 & 0 & 0 & 0\\
0 & 0 & 0 & 0 & 0 & 0 & \sigma_s & 0 & \sigma_{sc} & -k_{10} & 0 & 0\\
0 & 0 & 0 & 0 & 0 & 0 & \varphi_s & 0 & \varphi_{sc} & \varphi_q & -k_{11} & 0\\
0 & 0 & 0 & 0 & 0 & \psi_a & \psi_s & \psi_{ac} & \psi_{sc} & \psi_q & \psi_h & -k_{12}
\end{pmatrix},$$

where,

$$J_1 = \frac{(1-e\,m)\,\beta\,k_2\,k_3}{k_1\,k_2},\ J_2 = \frac{(1-e\,m)\,\beta\,k_3\,\tau_3\,\Omega}{k_1\,k_2},\ J_3 = \frac{(1-e\,m)\,\beta\,(1-\epsilon)\,\xi_s\,(k_2+\theta_1\,\Omega)}{k_1\,k_2},$$
$$\text{and } J_4 = \frac{(1-e\,m)\,\beta\,\{k_2\,k_3+\tau_3\,\Omega\,k_3+(1-\epsilon)\,\xi_s\,(k_2+\theta_1\,\Omega)\}}{k_1\,k_2}.$$

Now consider $\mathscr{R}_c = 1$ and $\beta = \beta^*$ is a bifurcation parameter. Thus we get

$$\beta = \beta^* = \frac{N^{**}}{(1-e\,m)\left\{S^*+\tau_3\,S_c^*+(1-\epsilon)\,S_v^*+\alpha\,R^*\right\}(\eta_e\,B_e+\eta_a\,B_a+B_s+\mathscr{T}_1\,B_{ac}+\mathscr{T}_2\,B_{sc})}.$$

The Jacobian $J(\mathscr{E}_0)$ of (14) with $\beta = \beta^*$ (β^* calculated at the DFE, $\mathscr{E}_0$), denoted by J_{β^*}, has a simple zero eigenvalue (with all other eigenvalues having negative real part). Hence, center manifold theory (Carr, 2012, Castillo-Chavez and Song, 2004), can be applied.

Eigenvectors of $J_{\beta^*} = J(\mathscr{E}_0)|_{\beta=\beta^*}$:

When $\mathscr{R}_c = 1$, a right eigenvector corresponding to the zero eigenvalue of the jacobian (J_{β^*}) is given by $w = [w_1, w_2, w_3, w_4, w_5, w_6, w_7, w_8, w_9, w_{10}, w_{11}, w_{12}]^T$, where.

$$w_1 = \frac{-(\eta_e J_1 w_5 + \eta_a J_1 w_6 + J_1 w_7 + \tau_1 J_1 w_8 + \tau_2 J_1 w_9)}{k_1},$$
$$w_2 = \frac{\Omega w_1 - (\eta_e J_2 w_5 + \eta_a J_2 w_6 + J_2 w_7 + \tau_1 J_2 w_8 + \tau_2 J_2 w_9)}{k_2},$$
$$w_3 = \frac{\xi_s w_1 + \theta_1 \xi_s w_2 + \theta_2 \xi_s w_{12} - (\eta_e J_3 w_5 + \eta_a J_3 w_6 + J_3 w_7 + \tau_1 J_3 w_8 + \tau_2 J_3 w_9)}{k_3},$$
$$w_4 = \frac{k_5 w_5}{\sigma_1},\ w_5 = w_5,\ w_6 = \frac{d_1 \sigma_2 w_5}{k_6},\ w_7 = \frac{d_2 \sigma_2 w_5}{k_7},\ w_8 = \frac{d_3 \sigma_2 w_5}{k_8},\ w_9 = \frac{(1-d)\sigma_2 w_5}{k_9},$$
$$w_{10} = \frac{\sigma_s w_7 + \sigma_{sc} w_9}{k_{10}},\ w_{11} = \frac{\varphi_s w_7 + \varphi_{sc} w_9 + \varphi_q w_{10}}{k_{11}},\ w_{12} = \frac{\psi_a w_6 + \psi_s w_7 + \psi_{ac} w_8 + \psi_{sc} w_9 + \psi_q w_{10} + \psi_h w_{11}}{k_{12}}.$$

Further, a left eigenvector of J_{β^*} corresponding to the zero eigenvalue is given by $v = [v_1, v_2, v_3, v_4, v_5, v_6, v_7, v_8, v_9, v_{10}, v_{11}, v_{12}]$
where.

$$v_1 = v_2 = v_3 = v_{10} = v_{11} = v_{12} = 0,\quad v_4 = v_4,$$
$$v_5 = \frac{\eta_e J_4 v_4 + d_1 \sigma_2 v_6 + d_2 \sigma_2 v_7 + d_3 \sigma_2 v_8 + (1-d)\sigma_2 v_9}{k_5},$$
$$v_6 = \frac{\eta_a J_4 v_4}{k_6},\ v_7 = \frac{J_4 v_4}{k_7},\ v_8 = \frac{\tau_1 J_4 v_4}{k_8},\ v_9 = \frac{\tau_2 J_4 v_4}{k_9}.$$

Computations of *a* and *b*:
The expression for a and b from Carr (2012), Castillo-Chavez and Song (2004) is:
$a = \sum_{k,i,j=1}^{n} v_k w_i w_j \frac{\partial^2 f_k}{\partial x_i \partial x_j}(\mathscr{E}_0, \beta^*)$,
and $b = \sum_{k,i=1}^{n} v_k w_i \frac{\partial^2 f_k}{\partial x_i \partial \beta}(\mathscr{E}_0, \beta^*)$,
which becomes

$$\begin{aligned} a = {} & \frac{1}{\Lambda(\Omega k_3 + \Omega\theta_1\xi_s + k_2 k_3 + k_2\xi_s)^2}\{2(1-em)\beta k_1 k_2 k_3(\eta_a w_6 + \eta_e w_5 + \tau_1 w_8 + \tau_2 w_9 + w_7)(+\Omega\nu_4 w_1 k_3 - \Omega\nu_4 w_2\theta_1\xi_s \\ & + \Omega\nu_4 w_3 k_3 - \Omega\nu_4 w_4\theta_1\xi_s - \Omega\nu_4 w_5\theta_1\xi_s - \Omega\nu_4 w_6\theta_1\xi_s + \Omega\epsilon\nu_4 w_7\theta_1\xi_s - \Omega k_3\tau_3\nu_4 w_7 + \epsilon k_2\nu_4 w_7\xi_s + \epsilon\nu_4 w_1\xi_s k_2 + \epsilon\nu_4 w_2\xi_s k_2 \\ & - \epsilon\nu_4 w_3 k_2 k_3 + \epsilon\nu_4 w_4\xi_s k_2 + \epsilon\nu_4 w_5\xi_s k_2 + \epsilon\nu_4 w_6\xi_s k_2 + \epsilon\nu_4 w_8\xi_s k_2 + \epsilon\nu_4 w_9\xi_s k_2 + \epsilon\nu_4 w_{12}\xi_s k_2 + \nu_4 w_2\xi_s k_2\tau_3 + \nu_4 w_2 k_2 k_3\tau_3 \\ & + \Omega\alpha\nu_4 w_{12}\xi_c + \Omega\alpha\nu_4 w_{12} k_3 + \Omega\epsilon\nu_4 w_1\theta_1\xi_s + \Omega\epsilon\nu_4 w_2\theta_1\xi_s - \Omega\epsilon\nu_4 w_3 k_3 + \Omega\epsilon\nu_4 w_4\theta_1\xi_s + \Omega\epsilon\nu_4 w_6\theta_1\xi_s + \Omega\epsilon\nu_4 w_8\theta_1\xi_s \\ & + \Omega\epsilon\nu_4 w_9\theta_1\xi_s + \Omega\epsilon\nu_4 w_{12}\theta_1\xi_s - \Omega\nu_4 w_1 k_3\tau_3 + \Omega\nu_4 w_2\theta_1\xi_s\tau_3 - \Omega\nu_4 w_3 k_3\tau_3 - \Omega\nu_4 w_4 k_3\tau_3 - \Omega\nu_4 w_5 k_3\tau_3 - \Omega\nu_4 w_6 k_3\tau_3 \\ & - \Omega\nu_4 w_8 k_3\tau_3 - \Omega\nu_4 w_9 k_3\tau_3 - \Omega\nu_4 w_{12} k_3\tau_3 + \alpha\nu_4 w_{12}\xi_s k_2 + \alpha\nu_4 w_{12} k_2 k_3 - \Omega\nu_4 w_8\theta_1\xi_s - \Omega\nu_4 w_9\theta_1\xi_s - \Omega\nu_4 w_{12}\xi_c \\ & - \nu_4 w_2\xi_s k_2 - \nu_4 w_2 k_2 k_3 - \nu_4 w_4\xi_s k_2 - \nu_4 w_4 k_2 k_3 - \nu_4 w_5\xi_s k_2 - \nu_4 w_5 k_2 k_3 - \nu_4 w_6\xi_s k_2 - \nu_4 w_6 k_2 k_3 - \nu_4 w_8\xi_s k_2 - \nu_4 w_8 k_2 k_3 \\ & - \nu_4 w_9\xi_s k_2 - \nu_4 w_9 k_2 k_3 - \nu_4 w_{12}\xi_s k_2 - \nu_4 w_{12} k_2 k_3 + \Omega\epsilon\nu_4 w_5\theta_1\xi_s - \Omega\nu_4 w_7\theta_1\xi_s - k_2 k_3\nu_4 w_7 - k_2 k_3\nu_4 w_7\xi_s)\}, \end{aligned}$$

$$\begin{aligned} b = {} & \frac{(1-em)}{(\Omega k_3 + \Omega\theta_1\xi_s + k_2 k_3 + k_2\xi_s)}(\eta_a w_6 + \eta_e w_5 + \tau_1 w_8 + \tau_2 w_9 + w_7)(\Omega\epsilon\nu_3\theta_1\xi_s - \Omega\epsilon\nu_4\theta_1\xi_s - \Omega k_3\tau_3\nu_2 + \Omega k_3\tau_3\nu_4 + \epsilon k_2\nu_3\xi_s \\ & - \epsilon k_2\nu_4\xi_s - \Omega\nu_3\theta_1\xi_s + \Omega\nu_4\theta_1\xi_s - k_2 k_3\nu_1 + k_2 k_3\nu_4 - k_2\nu_3\xi_s + k_2\nu_4\xi_s). \end{aligned}$$

Hence according to Theorem 4.1 of Castillo-Chavez and Song (2004), it follows that model (2) will exhibit backward bifurcation at $\mathscr{R}_c = 1$ whenever $a > 0$ and $b > 0$. In this case with $\alpha = 10$ and all other parameters as given in Table 2, we have $a = 0.00002083149795 > 0$ and $b = 0.4997487034 > 0$. Thus backward bifurcation phenomenon occurs at $\mathscr{R}_c = 1$. This is shown in the figure (Fig. 2) below.

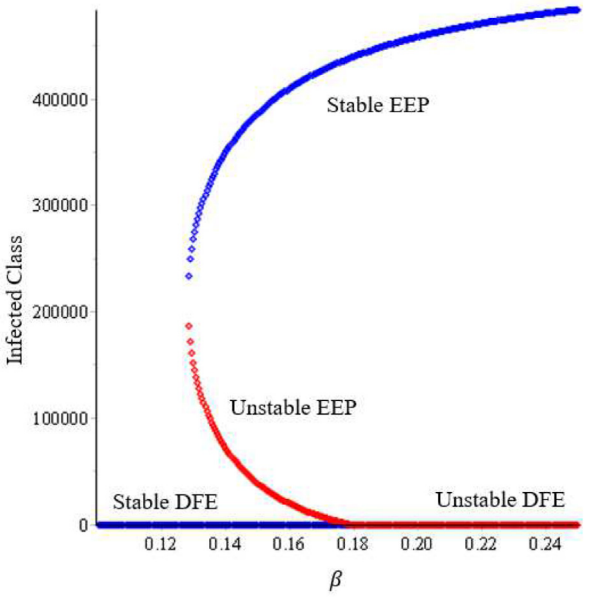

Fig. 2. Backward bifurcation diagram of model (2).

4. Dynamics of the model considering no re-infection

Now we will discuss the cases when there is no re-infection.

4.1. Global stability of DFE with $\alpha = 0$

Theorem 2. *The DFE of the COVID-19 model* (2) *with* $\alpha = 0$, *given by* $\mathscr{E}_0$, *is globally asymptotically stable (GAS) whenever* $\mathscr{R}_c \leq 1$.

Proof. We consider the following linear Lyapunov function:

$$\mathscr{L} = \ell_1 E_1 + \ell_2 E_2 + \ell_3 I_a + \ell_4 I_s + \ell_5 I_{ac} + \ell_6 I_{sc},$$

where,

$$\ell_1 = \frac{\sigma_1}{k_4 k_5 k_6 k_7 k_8 k_9}[\eta_e k_6 k_7 k_8 k_9 + k_7 k_8 k_9 d_1 \sigma_2 \eta_a + k_6 k_8 k_9 d_2 \sigma_2 \eta_a + k_6 k_7 k_9 d_3 \sigma_2 \mathscr{T}_1 + k_6 k_7 k_8 (1-d) \sigma_2 \mathscr{T}_2],$$

$$\ell_2 = \frac{k_4}{\sigma_1}\ell_1, \ \ell_3 = \frac{\eta_a k_9}{k_6 \mathscr{T}_2}, \ \ell_4 = \frac{k_9}{k_7 \mathscr{T}_2}, \ \ell_5 = \frac{\mathscr{T}_1 k_9}{k_8 \mathscr{T}_2}, \ \ell_6 = 1.$$

Differentiating the above Lyapunov function we have the following

$$\begin{aligned}\dot{\mathscr{L}} &= \ell_1 \dot{E_1} + \ell_2 \dot{E_2} + \ell_3 \dot{I_a} + \ell_4 \dot{I_s} + \ell_5 \dot{I_{ac}} + \ell_6 \dot{I_{sc}} \\ &= \ell_1 \{\lambda S + \mathscr{T}_3 \lambda S_c + (1-\epsilon_v)\lambda S_v + \alpha \lambda R - k_4 E_1\} + \ell_2 (\sigma_1 E_1 - k_5 E_2) + \ell_3 (d_1 \sigma_2 E_2 - k_6 I_a) + \\ &\quad \ell_4 (d_2 \sigma_2 E_2 - k_7 I_s) + \ell_5 (d_3 \sigma_2 E_2 - k_8 I_{ac}) + \ell_6 \{(1-d)\sigma_2 E_2 - k_9 I_{sc}\}\end{aligned}$$

$$= (-\ell_1 k_4 + \ell_2 \sigma_1) E_1 + \left\{ \ell_1 \eta_e \frac{\beta(1-em)(S^* + \tau_3 S_c^* + (1-\epsilon) S_v^*)}{N^{**}} - \ell_2 k_5 + \ell_3 d_1 \sigma_2 + \ell_4 d_2 \sigma_2 + \ell_5 d_3 \sigma_2 + \ell_6 (1-d) \sigma_2 \right\} E_2 +$$
$$\left\{ \ell_1 \eta_a \frac{\beta(1-em)(S^* + \tau_3 S_c^* + (1-\epsilon) S_v^*)}{N^{**}} - \ell_3 k_6 \right\} I_a + \left\{ \ell_1 \frac{\beta(1-em)(S^* + \tau_3 S_c^* + (1-\epsilon) S_v^*)}{N^{**}} - \ell_4 k_7 \right\} I_s +$$
$$\left\{ \ell_1 \tau_1 \frac{\beta(1-em)(S^* + \tau_3 S_c^* + (1-\epsilon) S_v^*)}{N^{**}} - \ell_5 k_8 \right\} I_{ac} + \left\{ \ell_1 \tau_2 \frac{\beta(1-em)(S^* + \tau_3 S_c^* + (1-\epsilon) S_v^*)}{N^{**}} - \ell_6 k_9 \right\} I_{sc}$$

After some rigorous calculation it can be shown that

$$\dot{\mathscr{L}} \leq \frac{\eta_e k_9}{\tau_2} \left(\frac{\tau_2}{k_9} \mathscr{R}_c - 1 \right) E_2 + \frac{\eta_a k_9}{\tau_2} \left(\frac{\tau_2}{k_9} \mathscr{R}_c - 1 \right) I_a + \frac{k_9}{\tau_2} \left(\frac{\tau_2}{k_9} \mathscr{R}_c - 1 \right) I_s + \frac{\tau_1 k_9}{\tau_2} \left(\frac{\tau_2}{k_9} \mathscr{R}_c - 1 \right) I_{ac} + k_9 \left(\frac{\tau_2}{k_9} \mathscr{R}_c - 1 \right) I_{sc}.$$

Thus

$$\begin{aligned} \dot{\mathscr{L}} &\leq \frac{k_9}{\tau_2} \left(\frac{\tau_2}{k_9} \mathscr{R}_c - 1 \right) (\eta_e E_2 + \eta_a I_a + I_s + \mathscr{T}_1 I_{ac} + \mathscr{T}_2 I_{sc}) \\ &= \frac{\lambda N^{**} k_9}{\beta (1 - e m) \tau_2} \left(\frac{\tau_2}{k_9} \mathscr{R}_c - 1 \right) \\ &< 0 \quad \text{for} \quad \mathscr{R}_c \leq \frac{k_9}{\tau_2} < 1. \end{aligned}$$

Also $\dot{\mathscr{L}} = 0$ if and only if $E_2 = I_a = I_s = I_{ac} = I_{sc} = 0$. Hence $\dot{\mathscr{L}} \leq 0$. Therefore, $\mathscr{L}$ is a Lyapunov function on $\mathscr{D}$ and thus it follows by the LaSalle's invariance principle (LaSalle, 1976) that, the DFE of the model (2) is globally asymptotic stable whenever $\mathscr{R}_c \leq 1$. □

4.2. Endemic equilibrium point (EEP) with $\alpha = 0$

When $\alpha = 0$ equation (12) reduces to

$$f(\lambda^*) = M_4 \lambda^{*4} + M_3 \lambda^{*3} + M_2 \lambda^{*2} + M_1 \lambda^* + M_0 = 0. \tag{15}$$

where,

$$\begin{aligned} M_4 &= (1-\epsilon) A_1 (W_c k_{12} + W_r) + A_4 \tau_3 (1-\epsilon), \\ M_3 &= A_4 \tau_3 k_3 + (1-\epsilon) A_4 k_2 + (1-\epsilon) A_5 \tau_3 + A_7 + A_1 k_3 (W_c k_{12} + W_r) + (1-\epsilon) A_2 (W_c k_{12} + W_r) + A_4 \Omega (1-\epsilon) \\ &\quad - \beta (1-em)(\eta_e W_e + \eta_a W_a + W_s + \tau_1 W_{ac} + \tau_2 W_{sc}) A_1 (1-\epsilon) k_{12}, \\ M_2 &= A_4 k_2 k_3 + A_6 \tau_3 (1-\epsilon) + A_5 \tau_3 k_3 + A_5 (1-\epsilon) k_2 + A_8 + (1-\epsilon) A_3 (W_c k_{12} + W_r) + A_2 k_3 (W_c k_{12} + W_r) + A_4 \Omega k_3 + A_5 \Omega (1-\epsilon) \\ &\quad - \beta (1-em)(\eta_e W_e + \eta_a W_a + W_s + \tau_1 W_{ac} + \tau_2 W_{sc})(A_1 k_3 k_{12} + A_2 (1-\epsilon) k_{12}), \\ M_1 &= A_5 k_2 k_3 + A_6 \tau_3 k_3 + (1-\epsilon) k_2 A_6 + A_9 + A_3 k_3 W_c k_{12} + A_3 k_3 W_r + \Omega A_5 k_3 + \Omega A_6 (1-\epsilon) \\ &\quad - \beta (1-em)(\eta_e W_e + \eta_a W_a + W_s + \tau_1 W_{ac} + \tau_2 W_{sc})(A_2 k_3 k_{12} - A_3 (1-\epsilon) k_{12}), \\ M_0 &= \Omega A_6 k_3 + A_6 k_2 k_3 + A_{10} - A_3 \beta (1-em)(\eta_e W_e + \eta_a W_a + W_s + \tau_1 W_{ac} + \tau_2 W_{sc}) k_3 k_{12}, \end{aligned}$$

where A_i's, $i = 1, 2, 3, \ldots, 10$ are the expressions from subsection 3.3 with $\alpha = 0$.

4.2.1. Local asymptotic stability of endemic equilibrium point (EEP) with $\alpha = 0$

Using the parameter values as given in Table 2 with $\alpha = 0$, it can be shown that $\mathscr{R}_c > 1$ and out of the four roots, one root is real positive, one root is real negative and other two roots are complex. So there exists a unique endemic equilibrium of system (2). Again using the same parameter values in the expression of a and b, we get $a = -0.000001860809076 < 0$ and $b = 0.4997487034 > 0$. Thus according to the Center Manifold Theorem (Castillo-Chavez and Song, 2004), this unique endemic equilibrium is locally asymptotically stable when $\mathscr{R}_c > 1$.

4.2.2. Global asymptotic stability of EEP with $\alpha = 0$

Theorem 3. *The EEP of the model* (2) *with no re-infection* ($\alpha = 0$) *is globally asymptotically stable (GAS) whenever* $\mathscr{R}_c > 1$.

The graph-theoretic approach discussed in Shuai and Driessche (2013) will be used to construct a Lyapunov function and to prove this theorem. Using Theorem 3.3, Theorem 3.4 and Theorem 3.5 of Shuai and Driessche (2013), the Lyapunov function can be constructed as follows:

Proof. The following Lyapunov function is considered:

$$\mathscr{L}_1 = \left(S - S^* - S^* \ln \frac{S}{S^*}\right) + \left(S_c - S_c^* - S_c^* \ln \frac{S_c}{S_c^*}\right) + \left(S_v - S_v^* - S_v^* \ln \frac{S_v}{S_v^*}\right) + \left(E_1 - E_1^* - E_1^* \ln \frac{E_1}{E_1^*}\right),$$

$$\mathscr{L}_2 = E_2 - E_2^* - E_2^* \ln \frac{E_2}{E_2^*},\ \mathscr{L}_3 = I_a - I_a^* - I_a^* \ln \frac{I_a}{I_a^*},\ \mathscr{L}_4 = I_s - I_s^* - I_s^* \ln \frac{I_s}{I_s^*},\ \mathscr{L}_5 = I_{ac} - I_{ac}^* - I_{ac}^* \ln \frac{I_{ac}}{I_{ac}^*},$$

$$\mathscr{L}_6 = I_{sc} - I_{sc}^* - I_{sc}^* \ln \frac{I_{sc}}{I_{sc}^*}.$$

Differentiating with respect to t we get

$$\mathscr{L}_1' \le \frac{\beta\,\eta_e\,(1-e\,m)\,E_2^*\left\{S^* + \tau_3\,S_c^* + (1-\epsilon)\,S_v^*\right\}}{N^{**}}\left(\frac{E_2}{E_2^*} - \ln\frac{E_2}{E_2^*} - \frac{E_1}{E_1^*} + \ln\frac{E_1}{E_1^*}\right) =: a_{12}\,G_{12}$$

$$+ \frac{\beta\,\eta_a\,(1-e\,m)\,I_a^*\left\{S^* + \tau_3\,S_c^* + (1-\epsilon)\,S_v^*\right\}}{N^{**}}\left(\frac{I_a}{I_a^*} - \ln\frac{I_a}{I_a^*} - \frac{E_1}{E_1^*} + \ln\frac{E_1}{E_1^*}\right) =: a_{13}\,G_{13}$$

$$+ \frac{\beta\,(1-e\,m)\,I_s^*\left\{S^* + \tau_3\,S_c^* + (1-\epsilon)\,S_v^*\right\}}{N^{**}}\left(\frac{I_s}{I_s^*} - \ln\frac{I_s}{I_s^*} - \frac{E_1}{E_1^*} + \ln\frac{E_1}{E_1^*}\right) =: a_{14}\,G_{14}$$

$$+ \frac{\beta\,\tau_1\,(1-e\,m)\,I_{ac}^*\left\{S^* + \tau_3\,S_c^* + (1-\epsilon)\,S_v^*\right\}}{N^{**}}\left(\frac{I_{ac}}{I_{ac}^*} - \ln\frac{I_{ac}}{I_{ac}^*} - \frac{E_1}{E_1^*} + \ln\frac{E_1}{E_1^*}\right) =: a_{15}\,G_{15}$$

$$+ \frac{\beta\,\tau_2\,(1-e\,m)\,I_{sc}^*\left\{S^* + \tau_3\,S_c^* + (1-\epsilon)\,S_v^*\right\}}{N^{**}}\left(\frac{I_{sc}}{I_{sc}^*} - \ln\frac{I_{sc}}{I_{sc}^*} - \frac{E_1}{E_1^*} + \ln\frac{E_1}{E_1^*}\right) =: a_{16}\,G_{16},$$

$$\mathscr{L}_2' \le \sigma_1\,E_1^*\left(\frac{E_1}{E_1^*} - \ln\frac{E_1}{E_1^*} - \frac{E_2}{E_2^*} + \ln\frac{E_2}{E_2^*}\right) =: a_{21}\,G_{21},$$

$$\mathscr{L}_3' \le d_1\,\sigma_2\,E_2^*\left(\frac{E_2}{E_2^*} - \ln\frac{E_2}{E_2^*} - \frac{I_a}{I_a^*} + \ln\frac{I_a}{I_a^*}\right) =: a_{31}\,G_{31},$$

$$\mathscr{L}_4' \le d_2\,\sigma_2\,E_2^*\left(\frac{E_2}{E_2^*} - \ln\frac{E_2}{E_2^*} - \frac{I_s}{I_s^*} + \ln\frac{I_s}{I_s^*}\right) =: a_{41}\,G_{41},$$

$$\mathscr{L}_5' \le d_3\,\sigma_2\,E_2^*\left(\frac{E_2}{E_2^*} - \ln\frac{E_2}{E_2^*} - \frac{I_{ac}}{I_{ac}^*} + \ln\frac{I_{ac}}{I_{ac}^*}\right) =: a_{51}\,G_{51},$$

$$\mathscr{L}_6' \le (1-d)\,\sigma_2\,E^*\left(\frac{E_2}{E_2^*} - \ln\frac{E_2}{E_2^*} - \frac{I_{sc}}{I_{sc}^*} + \ln\frac{I_{sc}}{I_{sc}^*}\right) =: a_{61}\,G_{61},$$

where.

$$a_{12} = \frac{\beta\,\eta_e\,(1-e\,m)\,E_2^*\left\{S^*+\tau_3\,S_c^*+(1-\epsilon)\,S_v^*\right\}}{N^{**}},\quad a_{13} = \frac{\beta\,\eta_a\,(1-e\,m)\,I_a^*\left\{S^*+\tau_3\,S_c^*+(1-\epsilon)\,S_v^*\right\}}{N^{**}},$$

$$a_{14} = \frac{\beta\,(1-e\,m)\,I_s^*\left\{S^*+\tau_3\,S_c^*+(1-\epsilon)\,S_v^*\right\}}{N^{**}},\quad a_{15} = \frac{\beta\,\tau_1\,(1-e\,m)\,I_{ac}^*\left\{S^*+\tau_3\,S_c^*+(1-\epsilon)\,S_v^*\right\}}{N^{**}},$$

$$a_{16} = \frac{\beta\,\tau_2\,(1-e\,m)\,I_{sc}^*\left\{S^*+\tau_3\,S_c^*+(1-\epsilon)\,S_v^*\right\}}{N^{**}},$$

$$a_{21} = \sigma_1\,E_1^*,\ a_{31} = d_1\,\sigma_2\,E_2^*,\ a_{41} = d_2\,\sigma_1\,E_2^*,\ a_{51} = d_3\,\sigma_2\,E_2^*,\ a_{61} = (1-d)\,\sigma_2\,E_2^*.$$

With the constants a_{ij} and $A = [a_{ij}]$, the following directed graph (Fig. 3) can be constructed. $\sum G_{ij} = 0$ along each of the cycles on the graph; for instances, $G_{41} + G_{14} = 0$, $G_{61} + G_{16} = 0$, and so on. Then by Theorem 3.5, there exist constants $c_i, i = 1, 2, \ldots, 6$ such that $\mathscr{L} = \sum_{i=1}^{6} c_i\,\mathscr{L}_i$ is a Lyapunov function for equation (2). To find the constants c_i we use Theorem 3.3 and Theorem 3.4. $d^+(2) = 1$ we have $c_2\,a_{21} = c_1\,a_{12}$.

Hence setting $c_1 = 1$ we get $c_2 = \frac{\beta\,(1-e\,m)\left\{S^*+\tau_3\,S_c^*+(1-\epsilon)\,S_v^*\right\}\,\eta_e\,E_2^*}{\sigma_1\,E_1^*\,N^{**}}$ $d^+(3) = 1$ implies $c_3\,a_{31} = c_1\,a_{13}$.

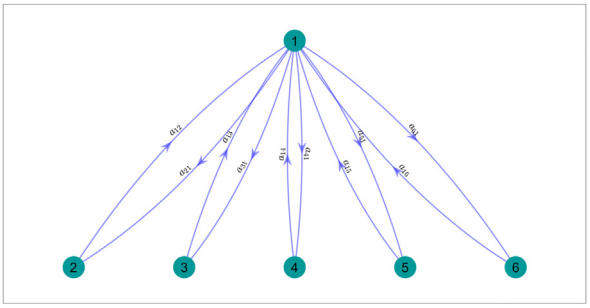

Fig. 3. Directed graph of system (2).

Hence setting $c_1 = 1$ we get $c_3 = \frac{\beta\,(1-e\,m)\,\{S^*+\tau_3\,S_c^*+(1-\epsilon)\,S_v^*\}\,\eta_a\,I_a^*}{d_1\,\sigma_2\,E_2^*\,N^{**}}$ $d^+(4) = 1$ implies $c_4\,a_{41} = c_1\,a_{14}$.

Hence setting $c_1 = 1$ we get $c_4 = \frac{\beta\,(1-e\,m)\,\{S^*+\tau_3\,S_c^*+(1-\epsilon)\,S_v^*\}\,I_s^*}{d_2\,\sigma_2\,E_2^*\,N^{**}}$ $d^+(5) = 1$ implies $c_5\,a_{51} = c_1\,a_{15}$.

Hence setting $c_1 = 1$ we get $c_5 = \frac{\beta\,(1-e\,m)\,\{S^*+\tau_3\,S_c^*+(1-\epsilon)\,S_v^*\}\,\tau_1\,I_{ac}^*}{d_3\,\sigma_2\,E_2^*\,N^{**}}$ $d^+(6) = 1$ implies $c_6\,a_{61} = c_1\,a_{16}$.

Hence setting $c_1 = 1$ we get $c_6 = \frac{\beta\,(1-e\,m)\,\{S^*+\tau_3\,S_c^*+(1-\epsilon)\,S_v^*\}\,\tau_2\,I_{sc}^*}{(1-d)\,\sigma_2\,E_2^*\,N^{**}}$.

Therefore with the functions $\mathscr{L}_i$, constants c_i given above and $\mathscr{K} = \frac{\beta\,(1-e\,m)\,\{S^*+\tau_3\,S_c^*+(1-\epsilon)\,S_v^*\}}{N^{**}}$, $\mathscr{L} = \mathscr{L}_1 + \mathscr{K}\frac{\eta_e\,E_2^*}{\sigma_1\,E_1^*}\mathscr{L}_2 + \mathscr{K}\frac{\eta_a\,I_a^*}{d_1\,\sigma_2\,E_2^*}\mathscr{L}_3 + \mathscr{K}\frac{I_s^*}{d_2\,\sigma_2\,E_2^*}\mathscr{L}_4 + \mathscr{K}\frac{\tau_1\,I_{ac}^*}{d_3\,\sigma_2\,E_2^*}\mathscr{L}_5 + \mathscr{K}\frac{\tau_2\,I_{sc}^*}{(1-d)\,\sigma_2\,E_2^*}\mathscr{L}_6$ is a Lyapunov function for (2). One can easily verify that for system (2) with this Lyapunov function and with $\mathscr{L}' = 0$ the largest invariant set will be the set $\mathscr{E}_1$. Hence, using LaSalle's invariance principle (LaSalle, 1976), we can say that $\mathscr{E}_1$ is globally asymptotically stable in the interior of $\mathscr{D}$. □

5. Optimal control

In this section, to control the spread of Covid-19, we reconsider the model (1) and formulate an optimal control problem with four control variables $u_1(t)$, $u_2(t)$, $u_3(t)$ and $u_4(t)$. The control $u_1(t)$ aims the efforts to increase awareness towards preventing COVID-19 infections by susceptible individuals (S), co-morbid susceptible humans (S_c), vaccination individuals (S_v) and recovered individuals (R) through various awareness program. Control $u_2(t)$ ensures the implementation of continuous vaccination, increase of vaccination rate and spread of vaccination program nationwide. $u_3(t)$ is COVID-19 detection control that represents the fraction of symptomatic individuals (I_s and I_{sc}) that are identified and quarantined for prevention of contacts with susceptible individuals. $u_4(t)$ represents the control that ensures better treatment and better care for the hospitalized individuals. Thus the revised model becomes:

$$\begin{aligned}
\dot{S} &= \Lambda - (1-u_1)\,\lambda\,S - \Omega\,S - \xi_s\,(1+u_2)\,S - \mu\,S,\\
\dot{S}_c &= \Omega\,S - (1-u_1)\,\mathscr{T}_3\,\lambda\,S_c - \theta_1\,\xi_s(1+u_2)\,S_c - \mu\,S_c,\\
\dot{S}_v &= \xi_s\,(1+u_2)\,S + \theta_1\,\xi_s\,(1+u_2)\,S_c + \theta_2\,\xi_s\,(1+u_2)\,R - (1-u_1)\,(1-\epsilon)\,\lambda\,S_v - k_3\,S_v,\\
\dot{E}_1 &= (1-u_1)\,\lambda\,(S+\mathscr{T}_3\,S_c + (1-\epsilon)\,S_v + \alpha\,R) - k_4\,E_1,\\
\dot{E}_2 &= \sigma_1\,E_1 - k_5\,E_2,\\
\dot{I}_a &= d_1\,\sigma_2\,E_2 - k_6\,I_a,\\
\dot{I}_s &= d_2\,\sigma_2\,E_2 - \sigma_s\,(1+u_3)\,I_s - (\psi_s + \varphi_s + \delta_s + \mu)\,I_s,\\
\dot{I}_{ac} &= d_3\,\sigma_2\,E_2 - k_8\,I_{ac},\\
\dot{I}_{sc} &= (1-d)\,\sigma_2\,E_2 - \sigma_{sc}\,(1+u_3)\,I_{sc} - (\psi_{sc} + \varphi_{sc} + \delta_{sc} + \mu)\,I_{sc},\\
\dot{Q} &= \sigma_s\,(1+u_3)\,I_s + \sigma_{sc}\,(1+u_3)\,I_{sc} - k_{10}\,Q,\\
\dot{H} &= \varphi_s\,I_s + \varphi_{sc}\,I_{sc} + \varphi_q\,Q - \psi_h(1+u_4)\,H - (\delta_h + \mu)\,H,\\
\dot{R} &= \psi_a\,I_a + \psi_s\,I_s + \psi_{ac}\,I_{ac} + \psi_{sc}\,I_{sc} + \psi_q\,Q + \psi_h(1+u_4)\,H - (1-u_1)\,\alpha\,\lambda\,R - \theta_2\,\xi_s\,(1+u_2)\,R - \mu\,R.
\end{aligned} \tag{16}$$

The objective of optimal control system is to find the controls that minimize the total infected individuals and the cost of implementing the controls, that is, to find the minimal values of u_1, u_2, u_3 and u_4 subject to the state system (16). In this paper, we consider a quadratic objective functional which includes pre-symptomatic individuals, asymptomatic infected individuals having no co-morbidity, symptomatic infected individuals having no co-morbidity, asymptomatic infected individuals having co-morbidity and symptomatic infected individuals having co-morbidity along with the four controls u_1, u_2, u_3 and u_4.

Quadratic objective functional is considered due to the fact that intervention is non-linear in its nature (Ndii and Adi, 2021). In fact, quadratic control is a common form of an objective functional in an optimal control problem and is frequently used in the literature (Ndii and Adi, 2021, Alemneh and Alemu, 2021, Kim et al., 2018, Shen et al., 2021, Majumder et al., 2022, Zamir et al., 2021, Omame et al., 2020, Li and Guo, 2022). Thus we have the following objective functional

$$J(u_1, u_2, u_3, u_4) = \int_0^T \left[D_1 E_2 + D_2 I_a + D_3 I_s + D_4 I_{ac} + D_5 I_{sc} + \frac{1}{2}\left(F_1 u_1^2 + F_2 u_2^2 + F_3 u_3^2 + F_4 u_4^2\right)\right] dt \tag{17}$$

The positive coefficients D_1, D_2, D_3, D_4, F_1, F_2, F_3 and F_4 are balancing weight parameters, while the controls u_1, u_2, u_3 and u_4 are bounded, Lebesgue integrable functions.

Theorem 1. *Let the set of controls for problem* (16) *be Lebesgue integrable functions (instead of just piecewise continuous functions) on* $0 \le t \le T$ *with values in* $\mathbb{R}$. *Then there exists an optimal control* $u^* = (u_1^*, u_2^*, u_3^*, u_4^* \in \mathscr{U})$ *such that* $J(u_1^*, u_2^*, u_3^*, u_4^*) = \min\{J(u_1, u_2, u_3, u_4) : u_1(t), u_2(t), u_3(t), u_4(t) \in \mathscr{U}\}$,

where $\mathscr{U} = \{(u_1, u_2, u_3, u_4) : u_i(t)$ *is measurable on* $[0, T],\ 0 \le u_i(t) \le 1,\ i = 1, 2, 3, 4\}$ is the closed set subject to the control system if the following conditions are satisfied (Fleming and Rishel, 2012).

1. *The set of state variables and controls is non-empty.*
2. *The control and state variables are non-negative values.*
3. *The control set* $\mathscr{U}$ *is convex and closed.*
4. *The integrand of the objective functional is convex on* $\mathscr{U}$.
5. *Successful responses on* $[0, T]$ *satisfy an a priori bound:*
   $|x(t; x_0, u(.))| \le \alpha,$ *for all* $u(.) \in \mathscr{U}(T), \quad 0 < t \le T$
   where $\alpha = \alpha(T)$ *is a constant depending only on T. This condition is implied by the followings:*

   (a) $|g(t, x_1, u)| \le C_1 (1 + |x| + |u|)$
   (b) $|g(t, x_1, u) - g(t, x, u)| \le C_2 |x_1 - x| (1 + |u|)$

6. *There exists constants* $C_3, C_4 > 0$ and C_5 *such that* $L(t; u_1; u_2; u_3; u_4)$ *satisfies*

   $$L(t; u_1; u_2; u_3; u_4) \ge C_3 + C_4 \left(|u_1|^2 + |u_2|^2 + |u_3|^2 + |u_4|^2\right)^{\frac{C_5}{2}}$$

Proof. Let us consider the following basic optimal control problem in the form of ordinary differential equation.
$\dot{x} = g(t, x(t), u(t)), \quad x(0) = x_0, \quad u(.) \in \mathscr{U}_m$ with associated cost $C[u(.)] = \int_0^T f(t, x(t), u(t))dt$,
where $x(t)$ represents state variable and $\mathscr{U}$ represents control and f, g are given continuous functions with values in $\mathbb{R}^n$ and $\mathbb{R}$.

1. Let $\mathscr{U}$ be the class of all admissible controls in time t, $0 < t \le T$. Obviously for some T, $\mathscr{U}(T)$ is non-empty, $\mathscr{U}(T) \neq \emptyset$, since we can't have an optimal control without at least one successful control. To prove that the set of controls is nonempty, we will use a simplified version of an existence theorem (Theorem 7.1.1) from Boyce and DiPrima (2020). Consider $S = x_1$, $S_c = x_2$, $S_v = x_3$, $E_1 = x_4$, $E_2 = x_5$, $I_a = x_6$, $I_s = x_7$, $I_{ac} = x_8$, $I_{sc} = x_9$, $Q = x_{10}$, $H = x_{11}$, and $R = x_{12}$, and thus in vector notation system (16) becomes $\frac{dX}{dt} = F(t; X)$, where $X = (x_1, x_2, x_3, x_4, x_5, x_6, x_7, x_8, x_9, x_{10}, x_{11}, x_{12})^T$ and $F = (f_1, f_2, f_3, f_4, f_5, f_6, f_7, f_8, f_9, f_{10}, f_{11}, f_{12})^T$. Let u_1, u_2, u_3, and u_4 are some constants. Since all parameters are constants and all x_i's are continuous, then all f_i's are also continuous ($i = 1, 2, \ldots, 12$). Additionally, the partial derivatives $\frac{\partial f_i}{\partial x_i}$, $i = 1, 2, \ldots, 12$ are also continuous. Therefore, there exists a unique solution $(S, S_c, S_v, E_1, E_2, I_a, I_s, I_{ac}, I_{sc}, Q, H, R)$ that satisfies the initial conditions. Thus, the set of controls and the corresponding state variables is nonempty and hence condition 1 is satisfied.
2. It is obvious that the set of state variables and controls are non-negative.
3. Let $u, v \in \mathscr{U}$ and $r \in [0, 1]$, then obviously $r u + (1 - r) v \ge 0$. Again $r u \le r$ and $(1 - r) v \le (1 - r)$

   Thus, $r u + (1 - r) v \le r + (1 - r) = 1$. Hence we have $0 \le r u + (1 - r) v \le 1$.
   Thus the control space

$$\mathscr{U} = \{(u_1, u_2, u_3, u_4) : (u_1, u_2, u_3, u_4) \text{ is measurable and } 0 \le u_{1_{\min}} \le u_1(t) \le u_{1_{\max}} \le 1,$$
$$0 \le u_{2_{\min}} \le u_2(t) \le u_{2_{\max}} \le 1, 0 \le u_{3_{\min}} \le u_3(t) \le u_{3_{\max}} \le 1, 0 \le u_{4_{\min}} \le u_4(t) \le u_{4_{\max}} \le 1\} \text{ is convex.}$$

4. The integrand of the objective functional is given by

$$\mathbb{L}(t; u_1; u_2; u_3; u_4) = D_1 E_2 + D_2 I_a + D_3 I_s + D_4 I_{ac} + D_5 I_{sc} + \tfrac{1}{2}(F_1 u_1^2 + F_2 u_2^2 + F_3 u_3^2 + F_4 u_4^2)$$

Here $\mathbb{L}$ is a twice differentiable function of many variables on the convex set $\mathscr{U}$ and let $\mathbb{H}$ denotes the Hessian of $\mathbb{L}$. We can determine the (strict) convexity of $\mathbb{L}$ by determining whether the Hessian is positive (definite) semi-definite. The second partial derivatives of $\mathbb{L}$ are.

$$\begin{array}{l}\mathbb{L}_{u_1u_1} = F_1,\ \mathbb{L}_{u_1u_2} = 0,\ \mathbb{L}_{u_1u_3} = 0,\ \mathbb{L}_{u_1u_4} = 0,\\ \mathbb{L}_{u_2u_1} = 0,\ \mathbb{L}_{u_2u_2} = F_2,\ \mathbb{L}_{u_2u_3} = 0,\ \mathbb{L}_{u_2u_4} = 0,\\ \mathbb{L}_{u_3u_1} = 0,\ \mathbb{L}_{u_3u_2} = 0,\ \mathbb{L}_{u_3u_3} = F_3,\ \mathbb{L}_{u_3u_4} = 0,\\ \mathbb{L}_{u_4u_1} = 0,\ \mathbb{L}_{u_4u_2} = 0,\ \mathbb{L}_{u_4u_3} = 0,\ \mathbb{L}_{u_4u_4} = F_4,\end{array}$$

So its Hessian is.

$$\mathbb{H} = \begin{pmatrix} F_1 & 0 & 0 & 0 \\ 0 & F_2 & 0 & 0 \\ 0 & 0 & F_3 & 0 \\ 0 & 0 & 0 & F_4 \end{pmatrix},$$

The Hessian is positive definite and hence $\mathscr{L}$ is strictly convex.

5. Consider $g(t, x, u) = \alpha(t, x) + u\,\beta(t, x)$ and assume that $g(t, x, u)$ is of class C^1 and $|g(t, 0, 0)| \le C$, $|g_x(t, x, u)| \le C(1 + |u|)$, $|g_u(t, x, u)| \le C$ for some constant C.

Applying Mean Value Theorem we get.

$$\frac{g(t, x_1, u) - g(t, x, u)}{x_1 - x} = g_x(t, x, u) \Rightarrow g(t, x_1, u) - g(t, x, u) = (x_1 - x)\, g_x(t, x, u)$$
$$|g(t, x_1, u) - g(t, x, u)| = |x_1 - x|\,|g_x(t, x, u)| \le |x_1 - x|\, C\,(1 + |u|)$$

Therefore, $|g(t, x_1, u) - g(t, x, u)| \le C\,|x_1 - x|\,(1 + |u|)$

$$\frac{g(t, x, 0) - g(t, 0, 0)}{x} = g_x(t, x, 0) \Rightarrow g(t, x, 0) - g(t, 0, 0) = x\, g_x(t, x, 0)$$
$$|g(t, x, 0) - g(t, 0, 0)| = |x\, g_x(t, x, 0)|$$
$$|g(t, x, 0)| - |g(t, 0, 0)| \le |x||g_x(t, x, 0)| \quad as\ |g(t, x, 0)| - |g(t, 0, 0)| \le |g(t, x, 0) - g(t, 0, 0)|$$
$$|g(t, x, 0)| - C \le C\,|x| \Rightarrow |g(t, x, 0)| \le C\,|x| + C \Rightarrow |g(t, x, 0)| \le C\,(1 + |x|)$$

Now.

$$\frac{g(t, x, u) - g(t, x, 0)}{u} = g_u(t, x, u) \Rightarrow g(t, x, u) - g(t, x, 0) = u\, g_u(t, x, u)$$
$$|g(t, x, u) - g(t, x, 0)| = |u\, g_x(t, x, u)| \Rightarrow |g(t, x, u)| - |g(t, x, 0)| \le |u|\,|g_x(t, x, u)|$$
$$|g(t, x, u)| - C\,(1 + |x|) \le C\,|u| \Rightarrow |g(t, x, u)| \le C\,|u| + C\,(1 + |x|)$$

Therefore, $|g(t, x, u)| \le C\,(1 + |x| + |u|)$.

6. The state variables being bounded,

let $C_3 = \min(D_1 E_2 + D_2 I_a + D_3 I_s + D_4 I_{ac} + D_5 I_{sc})$, $C_4 = \min\left(\frac{F_1}{2} + \frac{F_2}{2} + \frac{F_3}{2} + \frac{F_4}{2}\right)$, and $C_5 = 2$. Then it follows that $L(t; u_1; u_2; u_3; u_4)$ satisfies.

$L(t; u_1; u_2; u_3; u_4) \ge C_3 + C_4\left(|u_1|^2 + |u_2|^2 + |u_3|^2 + |u_4|^2\right)^{\frac{C_5}{2}}$ for all t with $0 \le t \le T$, x, x_1, u in $\mathbb{R}$. □

After establishing the existence of an optimal control, to obtain the necessary conditions for the optimal solution, we applied Pontryagin's maximum principle (Pontryagin, 1987) to the Hamiltonian $\mathscr{H}$ defined by

$$
\begin{aligned}
\mathscr{H} &= D_1 E_2 + D_2 I_a + D_3 I_s + D_4 I_{ac} + D_5 I_{sc} + \frac{1}{2}(F_1 u_1^2 + F_2 u_2^2 + F_3 u_3^2 + F_4 u_4^2) \\
&+g_1 \quad [\Lambda - (1-u_1)\lambda S - \Omega S - \xi_s (1+u_2) S - \mu S] \\
&+g_2 \quad [\Omega S - (1-u_1)\mathscr{T}_3 \lambda S_c - \theta_1 \xi_s (1+u_2) S_c - \mu S_c] \\
&+g_3 \quad [\xi_s (1+u_2) S + \theta_1 \xi_s (1+u_2) S_c + \theta_2 \xi_s (1+u_2) R - (1-u_1)(1-\epsilon)\lambda S_v - \mu S_v] \\
&+g_4 \quad [(1-u_1)\lambda (S + \mathscr{T}_3 S_c + (1-\epsilon) S_v + \alpha R) - k_4 E_1] \\
&+g_5 \quad [\sigma_1 E_1 - k_5 E_2] \\
&+g_6 \quad [d_1 \sigma_2 E_2 - k_6 I_a] \\
&+g_7 \quad [d_2 \sigma_2 E_2 - \sigma_s (1+u_3) I_s - (\psi_s + \varphi_s + \delta_s + \mu) I_s] \\
&+g_8 \quad [d_3 \sigma_2 E_2 - k_8 I_{ac}] \\
&+g_9 \quad [(1-d)\sigma_2 E_2 - \sigma_{sc}(1+u_3) I_{sc} - (\psi_{sc} + \varphi_{sc} + \delta_{sc} + \mu) I_{sc}] \\
&+g_{10} \quad [\sigma_s (1+u_3) I_s + \sigma_{sc}(1+u_3) I_{sc} - k_{10} Q] \\
&+g_{11} \quad [\varphi_s I_s + \varphi_{sc} I_{sc} + \varphi_q Q - \psi_h (1+u_4) H - (\delta_h + \mu) H] \\
&+g_{12} \quad [\psi_a I_a + \psi_s I_s + \psi_{ac} I_{ac} + \psi_{sc} I_{sc} + \psi_q Q + \psi_h (1+u_4) H - (1-u_1)\alpha\lambda R - \theta_2 \xi_s (1+u_2) R - \mu R],
\end{aligned} \tag{18}
$$

where g_i, $i = 1, 2, \ldots \ldots, 12$ are the adjoint variables.

Theorem 2. *Given an optimal control* $(u_1^*, u_2^*, u_3^*, u_4^*)$ *and corresponding state solutions* $S_1 = S, S_2 = S_c, S_3 = S_v, S_4 = E_1, S_5 = E_2, S_6 = I_a, S_7 = I_s, S_8 = I_{ac}, S_9 = I_{sc}, S_{10} = Q, S_{11} = H, S_{12} = R$ *of the corresponding state system* (16)*, there exists adjoint variables,* g_i, $i = 1, 2, \ldots \ldots, 12$ *satisfying*

$$
\frac{d g_i}{d t} = -\frac{\partial H}{\partial S_i}
$$

with transversality conditions $g_i(T) = 0$*, where,* $i = 1, 2, \ldots \ldots, 12$ *and control set* $(u_1^*, u_2^*, u_3^*, u_4^*)$ *characterized by*

$$
\begin{aligned}
u_1^* &= \max\left\{0,\ \min\left(1,\ \frac{(g_4 - g_1)\lambda S + (g_4 - g_2)\tau_3 \lambda S_c + (g_4 - g_3)(1-\epsilon)\lambda S_v + (g_4 - g_{12})\alpha\lambda R}{F_1}\right)\right\}, \\
u_2^* &= \max\left\{0,\ \min\left(1,\ \frac{(g_1 - g_3)\xi_s S + (g_2 - g_3)\theta_1 \xi_s S_c + (g_{12} - g_3)\theta_2 \xi_s R}{F_2}\right)\right\}, \\
u_3^* &= \max\left\{0,\ \min\left(1,\ \frac{(g_7 - g_{10})\sigma_s I_s + (g_9 - g_{10})\sigma_{sc} I_{sc}}{F_3}\right)\right\}, \\
u_4^* &= \max\left\{0,\ \min\left(1,\ \frac{(g_{11} - g_{12})\psi_h H}{F_4}\right)\right\}.
\end{aligned} \tag{19}
$$

Proof.

$$
\begin{aligned}
\frac{d g_1}{d t} &= -\frac{\partial \mathscr{H}}{\partial S} = g_1 \left\{(1-u_1)\lambda + (\Omega + \xi_s (1+u_2)) + (1-u_1) S \frac{-\lambda}{N^*}\right\} - g_2 \left\{\Omega - (1-u_1)\tau_3 S_c \frac{-\lambda}{N^*}\right\}, \\
&-g_3 \left\{(\xi_s (1+u_2) - (1-u_1)(1-\epsilon) S_v \frac{-\lambda}{N^*}\right\} - g_4 \left\{(1-u_1)\lambda - (1-u_1)(S + \mathscr{T}_3 S_c + (1-\epsilon) S_v + \alpha R) \frac{-\lambda}{N^*}\right\}, \\
&-g_{12} \left\{(1-u_1)\alpha R \frac{\lambda}{N^*}\right\},
\end{aligned}
$$

$$\frac{dg_2}{dt} = -\frac{\partial \mathscr{H}}{\partial S_c} = -g_1\left\{(1-u_1)\,S\,\frac{-\lambda}{N^*}\right\} + g_2\left\{(1-u_1)\,\tau_3\,\lambda + \theta_1\,\xi_s\,(1+u_2) - (1-u_1)\,\tau_3\,S_c\,\frac{\lambda}{N^*}\right\},$$
$$-g_3\left\{(\theta_1\,\xi_s\,(1+u_2) - (1-u_1)\,(1-\epsilon)\,S_v\,\frac{-\lambda}{N^*}\right\}) - g_4\left\{(1-u_1)\,\tau_3\,\lambda + (1-u_1)\,(S+\mathscr{T}_3\,S_c + (1-\epsilon)\,S_v + \alpha R)\,\frac{-\lambda}{N^*}\right\},$$
$$-g_{12}\left\{(1-u_1)\,\alpha R\,\frac{\lambda}{N^*}\right\},$$

$$\frac{dg_3}{dt} = -\frac{\partial \mathscr{H}}{\partial S_v} = g_1\left\{(1-u_1)\,S\,\frac{-\lambda}{N^*}\right\} + g_2\left\{(1-u_1)\,\tau_3\,S_c\,\frac{-\lambda}{N^*}\right\} + g_3\left\{(1-u_1)\,(1-\epsilon)\,\lambda - (1-u_1)\,(1-\epsilon)\,S_v\,\frac{\lambda}{N^*}\right\},$$
$$-g_4\left\{(1-u_1)\,(1-\epsilon)\,\lambda + (1-u_1)\,(S+\mathscr{T}_3\,S_c + (1-\epsilon)\,S_v + \alpha R)\,\frac{-\lambda}{N^*}\right\} - g_{12}\left\{(1-u_1)\,\alpha R\,\frac{\lambda}{N^*}\right\},$$

$$\frac{dg_4}{dt} = -\frac{\partial \mathscr{H}}{\partial E_1} = g_1\left\{(1-u_1)S\frac{-\lambda}{N^*}\right\} + g_2\left\{(1-u_1)\tau_3 S_c\frac{-\lambda}{N^*}\right\},$$
$$+g_3\left\{(1-u_1)(1-\epsilon)S_v\frac{-\lambda}{N^*}\right\} + g_4\left\{(1-u_1)(S+\mathscr{T}_3 S_c + (1-\epsilon)S_v + \alpha R)\frac{-\lambda}{N^*} - \sigma_1\right\} - g_5\sigma_1 + g_{12}\left\{(1-u_1)\alpha R\frac{\lambda}{N^*}\right\},$$

$$\frac{dg_5}{dt} = -\frac{\partial \mathscr{H}}{\partial E_2} = -D_1 + g_1\left\{(1-u_1)S\left(\frac{(1-em)\beta\eta_e}{N^*} - \frac{\lambda}{N^*}\right)\right\} + g_2\left\{(1-u_1)\tau_3 S_c\left(\frac{(1-em)\beta\eta_e}{N^*} - \frac{\lambda}{N^*}\right)\right\},$$
$$+g_3\left\{(1-u_1)(1-\epsilon)S_v\left(\frac{(1-em)\beta\eta_e}{N^*} - \frac{\lambda}{N^*}\right)\right\} - g_4\left\{(1-u_1)(S+\mathscr{T}_3 S_c + (1-\epsilon)S_v + \alpha R)\left(\frac{(1-em)\beta\eta_e}{N^*} - \frac{\lambda}{N^*}\right),\right.$$
$$+g_5(\sigma_2+\delta_e) - g_6 d_1\sigma_2 - g_7 d_2\sigma_2 - g_8 d_3\sigma_2 - g_9(1-d)\sigma_2 + g_{12}\left\{(1-u_1)\alpha R\left(\frac{(1-em)\beta\eta_e}{N^*} - \frac{\lambda}{N^*}\right),\right.$$

$$\frac{dg_6}{dt} = -\frac{\partial \mathscr{H}}{\partial I_a} = -D_2 + g_1\left\{(1-u_1)S\left(\frac{(1-em)\beta\eta_a}{N^*} - \frac{\lambda}{N^*}\right)\right\} + g_2\left\{(1-u_1)\tau_3 S_c\left(\frac{(1-em)\beta\eta_a}{N^*} - \frac{\lambda}{N^*}\right)\right\},$$
$$+g_3\left\{(1-u_1)(1-\epsilon)S_v\left(\frac{(1-em)\beta\eta_a}{N^*} - \frac{\lambda}{N^*}\right)\right\} - g_4\left\{(1-u_1)(S+\mathscr{T}_3 S_c + (1-\epsilon)S_v + \alpha R)\left(\frac{(1-em)\beta\eta_a}{N^*} - \frac{\lambda}{N^*}\right),\right.$$
$$+g_6(\psi_a+\delta_a) + g_{12}\left\{-\psi_a + (1-u_1)\alpha R\left(\frac{(1-em)\beta\eta_a}{N^*} - \frac{\lambda}{N^*}\right)\right\},$$

$$\frac{dg_7}{dt} = -\frac{\partial \mathscr{H}}{\partial I_s} = -D_3 + g_1\left\{(1-u_1)\,S\left(\frac{(1-em)\,\beta}{N^*} - \frac{\lambda}{N^*}\right)\right\} + g_2\left\{(1-u_1)\,\tau_3\,S_c\left(\frac{(1-em)\,\beta}{N^*} - \frac{\lambda}{N^*}\right)\right\},$$
$$+g_3\left\{(1-u_1)\,(1-\epsilon)\,S_v\left(\frac{(1-em)\,\beta}{N^*} - \frac{\lambda}{N^*}\right)\right\} - g_4\left\{(1-u_1)\,(S+\mathscr{T}_3\,S_c + (1-\epsilon)\,S_v + \alpha R)\left(\frac{(1-em)\,\beta}{N^*} - \frac{\lambda}{N^*}\right),\right.$$
$$+g_7(\sigma_s\,(1+u_3) + \psi_s + \varphi_s + \delta_s) - g_{10}\,\sigma_s\,(1+u_3) - g_{11}\,\varphi_s + g_{12}\left\{-\psi_s + (1-u_1)\,\alpha R\left(\frac{(1-em)\,\beta}{N^*} - \frac{\lambda}{N^*}\right)\right\},$$

$$\frac{dg_8}{dt} = -\frac{\partial \mathscr{H}}{\partial I_{ac}} = -D_4 + g_1\left\{(1-u_1)S\left(\frac{(1-em)\beta\tau_1}{N^*} - \frac{\lambda}{N^*}\right)\right\} + g_2\left\{(1-u_1)\tau_3 S_c\left(\frac{(1-em)\beta\tau_1}{N^*} - \frac{\lambda}{N^*}\right)\right\},$$
$$+g_3\left\{(1-u_1)(1-\epsilon)S_v\left(\frac{(1-em)\beta\tau_1}{N^*} - \frac{\lambda}{N^*}\right)\right\} - g_4\left\{(1-u_1)(S+\mathscr{T}_3 S_c + (1-\epsilon)S_v + \alpha R)\left(\frac{(1-em)\beta\tau_1}{N^*} - \frac{\lambda}{N^*}\right),\right.$$
$$+g_8(\psi_{ac}+\delta_{ac}) + g_{12}\left\{-\psi_{ac} + (1-u_1)\alpha R\left(\frac{(1-em)\beta\tau_1}{N^*} - \frac{\lambda}{N^*}\right)\right\},$$

$$\frac{dg_9}{dt} = -\frac{\partial \mathscr{H}}{\partial I_{sc}} = -D_5 + g_1\left\{(1-u_1)S\left(\frac{(1-em)\beta\tau_2}{N^*} - \frac{\lambda}{N^*}\right)\right\} + g_2\left\{(1-u_1)\tau_3 S_c\left(\frac{(1-em)\beta\tau_2}{N^*} - \frac{\lambda}{N^*}\right)\right\},$$
$$+g_3\left\{(1-u_1)(1-\epsilon)S_v\left(\frac{(1-em)\beta\tau_2}{N^*} - \frac{\lambda}{N^*}\right)\right\} - g_4\left\{(1-u_1)(S + \mathscr{T}_3 S_c + (1-\epsilon)S_v + \alpha R)\left(\frac{(1-em)\beta\tau_2}{N^*} - \frac{\lambda}{N^*}\right),\right.$$
$$\left.+g_9(\sigma_{sc}(1+u_3) + \psi_{sc} + \varphi_{sc} + \delta_{sc}) - g_{10}\sigma_{sc}(1+u_3) - g_{11}\varphi_{sc} + g_{12}\left\{-\psi_{sc} + (1-u_1)\alpha R\left(\frac{(1-em)\beta\tau_2}{N^*} - \frac{\lambda}{N^*}\right)\right\},\right.$$

$$\frac{dg_{10}}{dt} = -\frac{\partial \mathscr{H}}{\partial Q} = g_{10}(\psi_q + \varphi_q) - g_{11}\varphi_q - g_{12}\psi_q,$$

$$\frac{dg_{11}}{dt} = -\frac{\partial \mathscr{H}}{\partial H} = g_{11}(\psi_h(1+u_4) + \delta_h) - g_{12}\psi_h(1+u_4),$$

$$\frac{dg_{12}}{dt} = -\frac{\partial \mathscr{H}}{\partial R} = g_1\left\{(1-u_1)S\frac{-\lambda}{N^*}\right\} - g_2\left\{-(1-u_1)\tau_3 S_c\frac{-\lambda}{N^*}\right\},$$
$$-g_3\left\{(\theta_2\xi_s(1+u_2) - (1-u_1)(1-\epsilon)S_v\frac{-\lambda}{N^*}\right\} - g_4\left\{(1-u_1)\lambda\alpha + (1-u_1)(S + \mathscr{T}_3 S_c + (1-\epsilon)S_v + \alpha R)\frac{-\lambda}{N^*}\right\},$$
$$-g_{12}\left\{-(1-u_1)\alpha R\frac{-\lambda}{N^*} - (1-u_1)\alpha\lambda - \theta_2\xi_s(1+u_2)\right\}.$$

Now $\frac{\partial \mathscr{H}}{\partial u_i} = 0,\ i = 1, 2, 3, 4$ *implies*

$$\frac{\partial \mathscr{H}}{\partial u_1} = F_1 u_1 + \lambda S(g_1 - g_4) + \tau_3\lambda S_c(g_2 - g_4) + (1-\epsilon)\lambda S_v(g_3 - g_4) + \alpha\lambda R(g_{12} - g_4) = 0,$$
$$\frac{\partial \mathscr{H}}{\partial u_2} = F_2 u_2 + \xi_s S(g_3 - g_1) + \theta_1\xi_s S_c(g_3 - g_2) + \theta_2\xi_s R(g_3 - g_{12}) = 0,$$
$$\frac{\partial \mathscr{H}}{\partial u_3} = F_3 u_3 + \sigma_s I_s(g_{10} - g_7) + \sigma_{sc} I_{sc}(g_{10} - g_9) = 0,$$
$$\frac{\partial \mathscr{H}}{\partial u_4} = F_4 u_4 + \psi_h H(g_{12} - g_{11}) = 0.$$

Solving the above system we have

$$u_1^* = \frac{(g_4 - g_1)\lambda S + (g_4 - g_2)\tau_3\lambda S_c + (g_4 - g_3)(1-\epsilon)\lambda S_v + (g_4 - g_{12})\alpha\lambda R}{F_1},$$
$$u_2^* = \frac{(g_1 - g_3)\xi_s S + (g_2 - g_3)\theta_1\xi_s S_c + (g_{12} - g_3)\theta_2\xi_s R}{F_2},$$
$$u_3^* = \frac{(g_7 - g_{10})\sigma_s I_s + (g_9 - g_{10})\sigma_{sc} I_{sc}}{F_3},$$
$$u_4^* = \frac{(g_{11} - g_{12})\psi_h H}{F_4}.$$

Hence the set of controls satisfy (19). □

6. Numerical simulations

In this section we have used our model to carry out numerical simulations using base line parameter values as given in Table 2.

6.1. Data collection, data fitting and parameter estimation

Data relevant to our model has been collected from the official website (Worldometers, 2019). Some parameter values have been obtained from already existing literature. Other parameter values have been calculated using the MATLAB fminsearchbnd function to fit the real data with our model. The fitting results obtained from our model are shown in Fig. 4 and compared with the daily infected cases of the USA. This figure suggests that our estimated values are very close to the real data and hence are reliable. The simulation results are presented in magenta color for $\beta = 0.60$, green color for $\beta = 0.57$, blue color for $\beta = 0.62$ and red color for $\beta = 0.78$.

6.2. Global sensitivity and uncertainty analysis

Sensitivity and uncertainity analysis is discussed in this section to study the uncertainty of our model and to identify the most influential parameters those can control the COVID-19 transmission (Marino et al., 2008). Parameters whose PRCC values lie in the range $|\text{PRCC}| > 0.5$ and have p-values less than 0.01 are thought of as highly correlated with the response function (Blower and Dowlatabadi, 1994, pp. 229–243, Taylor, 1990). In order to perform PRCC analysis, we start with Latin Hyperbolic Sampling (LHS) of the model parameters. The LHS matrix containing the LHS parameters are obtained by uniform distribution. In this paper, for PRCC analysis the model is simulated 500 times and the model is run for 510 days.

6.3. Effect of various parameters on the transmission dynamics of Covid-19

Now we will discuss about the top ranked parameters those can control the spread of COVID-19 nationwide. Performing PRCC analysis for the variables I_s, I_{sc} and basic reproduction number ($\mathscr{R}_c$) (Figs. 5–7) it is seen that effective contact rate (β) is the most important parameter that has a impact on the dynamics of COVID-19. These figures depict that (β) is positively correlated with the response functions I_s, I_{sc} and $\mathscr{R}_c$. This implies that minimizing the contact rate (increasing social distance), we can control the spread of COVID-19. Fig. 8 deals with the simulation of the model with different values of the effective contact rate parameter (β). From this figure we can observe a significant decrease in the number of daily infected individuals, daily hospitalization cases and cumulative deaths with a reduction in effective contact rate and hence disease related complexity decreases.

Figs. 5–7 also show that e (mask efficacy) & m (mask coverage) are negatively correlated with the response functions I_s, I_{sc} and $\mathscr{R}_c$ which implies we can reduce the disease related complexity if highly efficacious face mask can be used by a greater number of population in the community. Numerical simulations are also performed to present the combined effect of face mask coverage and face mask efficacy on the transmission dynamics of COVID-19 (Fig. 9). This figure tells that an increase in the value of e & m can help reduce the number of daily infected individuals, daily hospitalization cases and cumulative deaths. As for example Fig. 9 (a) shows that when no face mask is used the peak value is 423391 but when 25% of total population uses face mask of 25% efficacy, peak value becomes 365698 which implies a 13.6% reduction in peak value. Further a 16% reduction is noticed when 50% of total population uses face mask of same efficacy. Again a 19% reduction is noticed when 75% of total population uses face mask of same efficacy. Fig. 9 (b) shows a 27.5% reduction in peak value when 25% of total population uses face mask of 50% efficacy. This figure also shows a 38% reduction in peak value when 50% of total population uses face mask of 50% efficacy. Further a 49% reduction is observed when 70% of total population uses face mask of 50% efficacy. Fig. 9 (c) shows a 41.5% reduction in peak value when 25% of total population uses face mask of 75% efficacy. This figure also shows a 61%

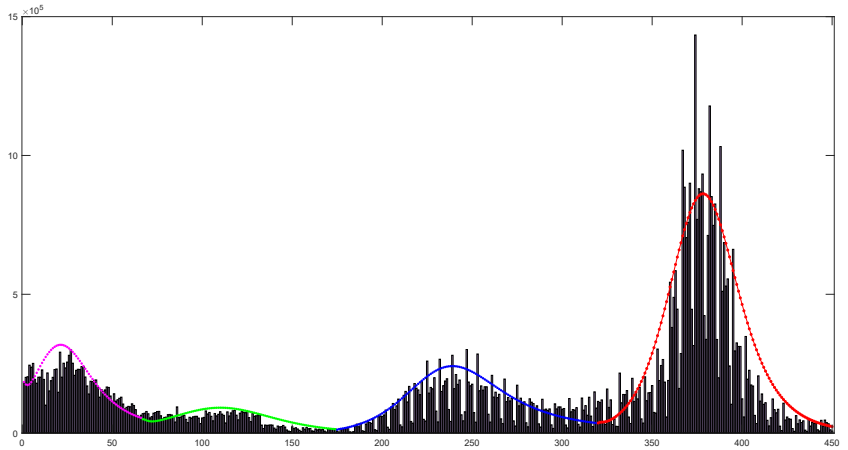

Fig. 4. Number of daily infected individuals in the U.S starting from December 13, 2020 to 19 March 2022, are plotted with the simulation results using the model (2).

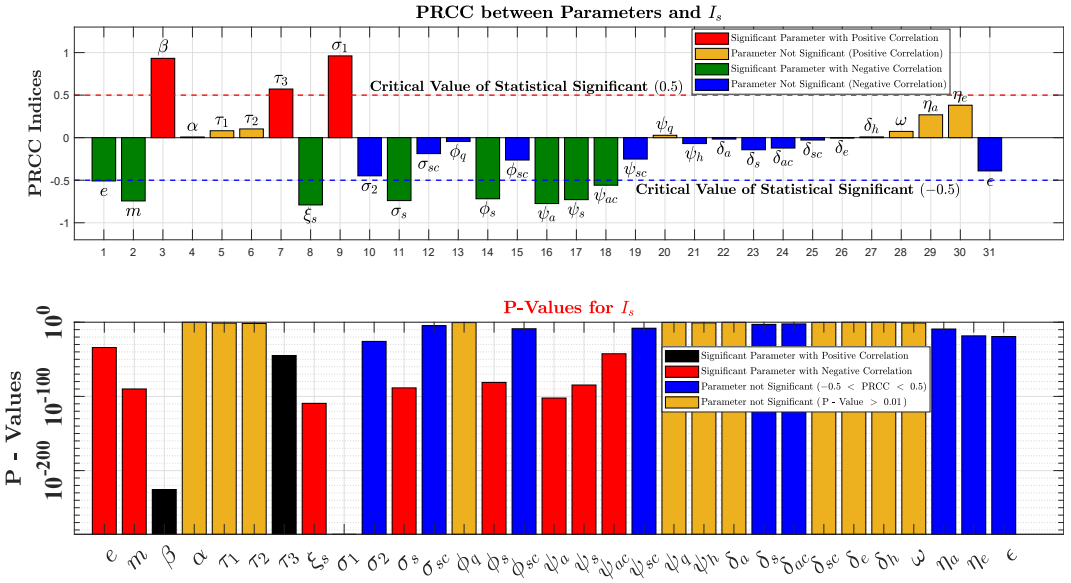

Fig. 5. PRCC analysis of the model (2) for the response function I_s.

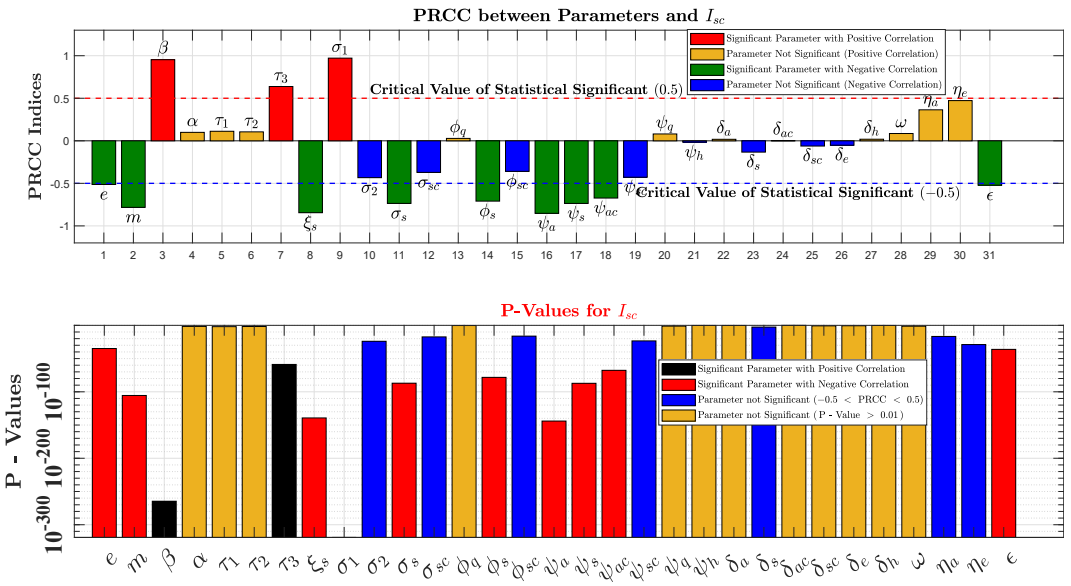

Fig. 6. PRCC analysis of the model (2) for the response function I_{sc}.

reduction in peak value when 50% of total population uses face mask of 75% efficacy. In short, we can say that when mask coverage and mask efficacy both increases peak value of daily infected cases decreases significantly. Similar results are observed for daily hospitalized cases and cumulative deaths.

Again it is evident from Figs. 5–7 that ξ_s is negatively correlated with the response functions I_s, I_{sc} and $\mathscr{R}_c$ which suggests that mass vaccination campaign can slow down the spread of COVID-19. This is shown graphically in Fig. 10. From this figure, it can be seen that number of daily infected individuals, hospitalized individuals and cumulative deaths decreases remarkably when vaccination rate is increased. For instance Fig. 10 (a) shows that when no vaccine is implemented, the peak of the daily infected cases is 405788. But when the vaccine coverage is increased to base line value, the peak value becomes 221946 which implies a 45.5% reduction in peak value. Again when the vaccination coverage is increased 30% from its base line value the

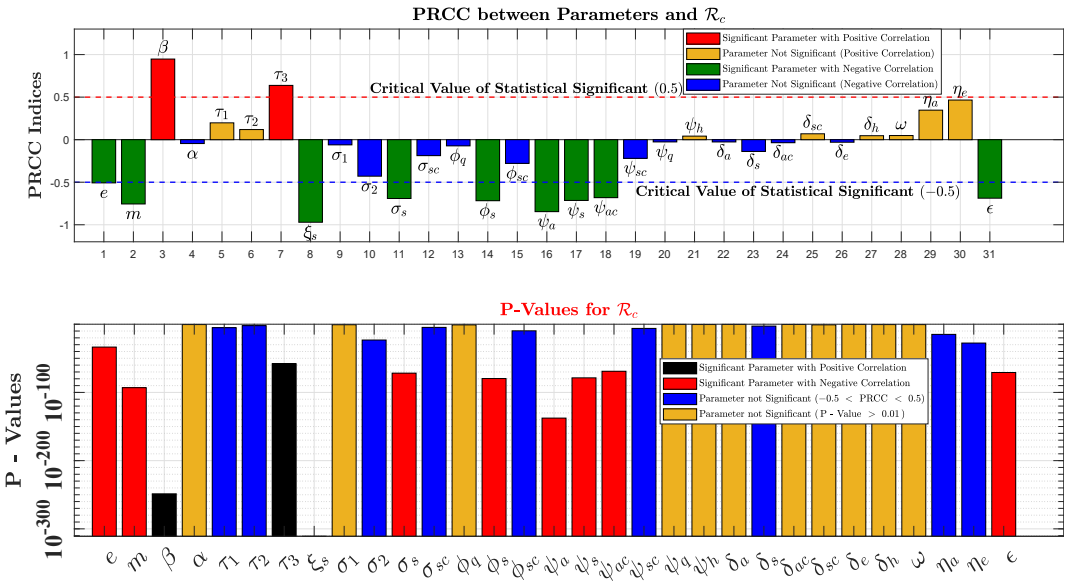

Fig. 7. PRCC analysis of the model (2) for the response function $\mathscr{R}_c$.

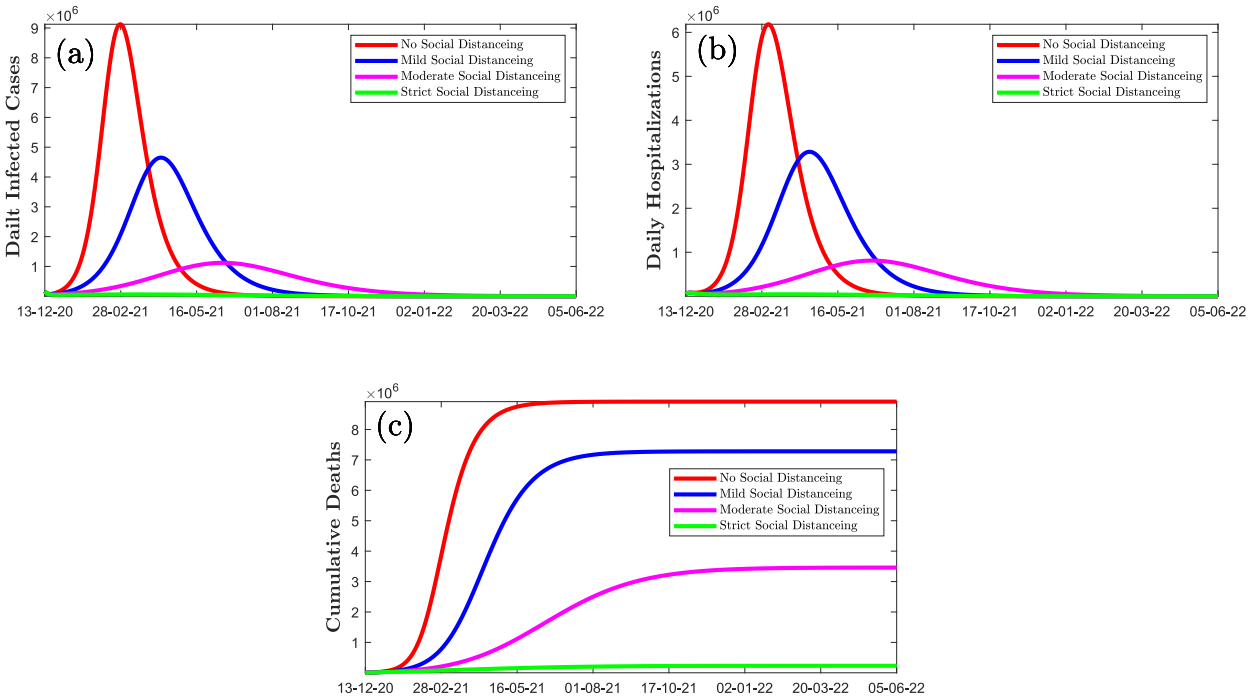

Fig. 8. Numerical results showing the impact of social distancing in controlling the transmission of COVID-19.

peak is reduced by 14%. Further a 12% reduction in the peak value is observed when the base line vaccine coverage is increased by 60%. Similar trends are observed for daily hospitalized case and cumulative deaths (Fig. 10 (b) and Fig. 10 (c)).

In model (2), parameter ϵ represents the efficacy of vaccine and from Figs. 5–7, it is clear that it has a large negative PRCC value which means that it has a negative impact on the spread of COVID-19. Thus vaccines with high efficacy can lead to the elimination of COVID-19 from the community. Fig. 11 supports this statement. This figure depicts that the more a vaccine is effective, the less is the number of daily infected individuals, hospitalized individuals, and cumulative death cases. For

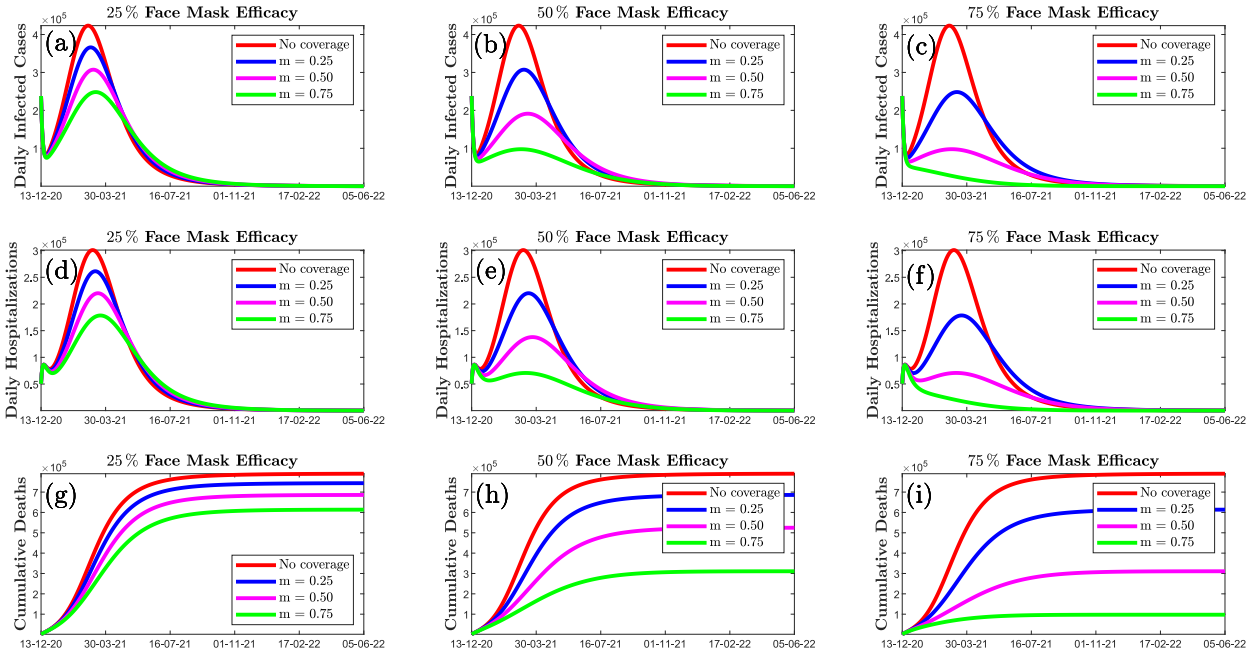

Fig. 9. Numerical results showing the combined effect of face mask coverage and mask efficacy in controlling the transmission of COVID-19.

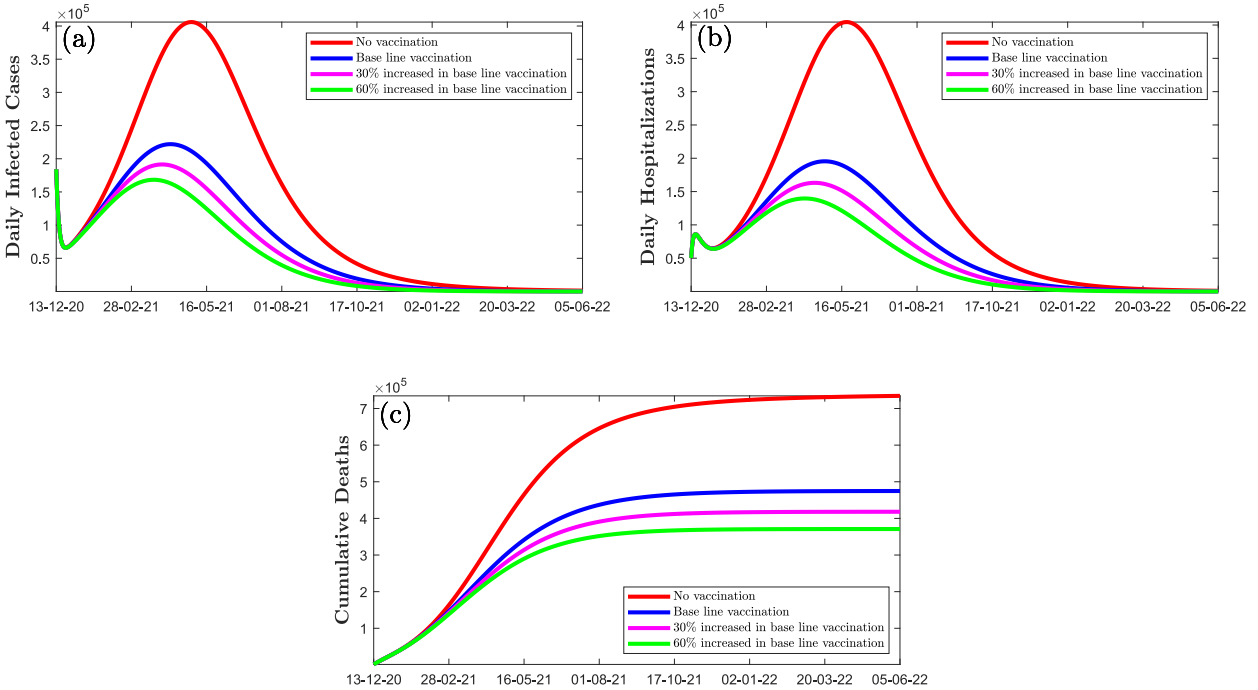

Fig. 10. Simulations of the model (2) showing the effect of vaccination on the transmission dynamics of COVID-19 with various vaccine coverage.

instance Fig. 11 (a) shows that when vaccine efficacy is 60%, the peak of the daily infected cases is 547309. But when the vaccine efficacy is 70%, the peak value becomes 423805 which implies a 23% reduction in peak value. Again when the efficacy increases to 80% the peak is reduced by 20%. Further a 18% reduction in the peak value is observed when the vaccine efficacy

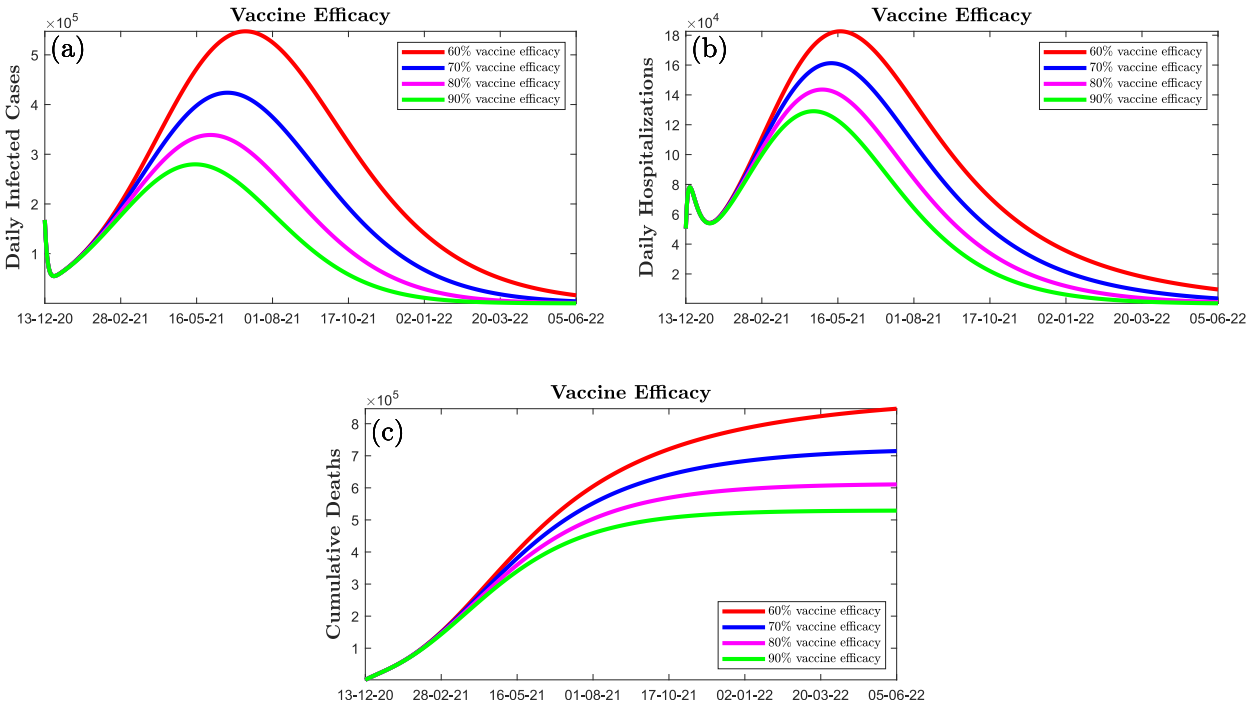

Fig. 11. Numerical results showing the effect of vaccine efficacy on the transmission dynamics of COVID-19.

increases to 90%. In short, we can say that the peak of the daily infected cases decreases remarkably when the vaccine efficacy increases. Similar trends are observed for daily hospitalized cases and cumulative deaths (Fig. 11 (b) and Fig. 11 (c)).

Fig. 12 (a) assesses the combined effect of face mask coverage and mask efficacy on the basic reproduction number by drawing contour plot of the reproduction number $\mathscr{R}_c$ as a function of mask coverage (m) and mask efficacy (e). This figure

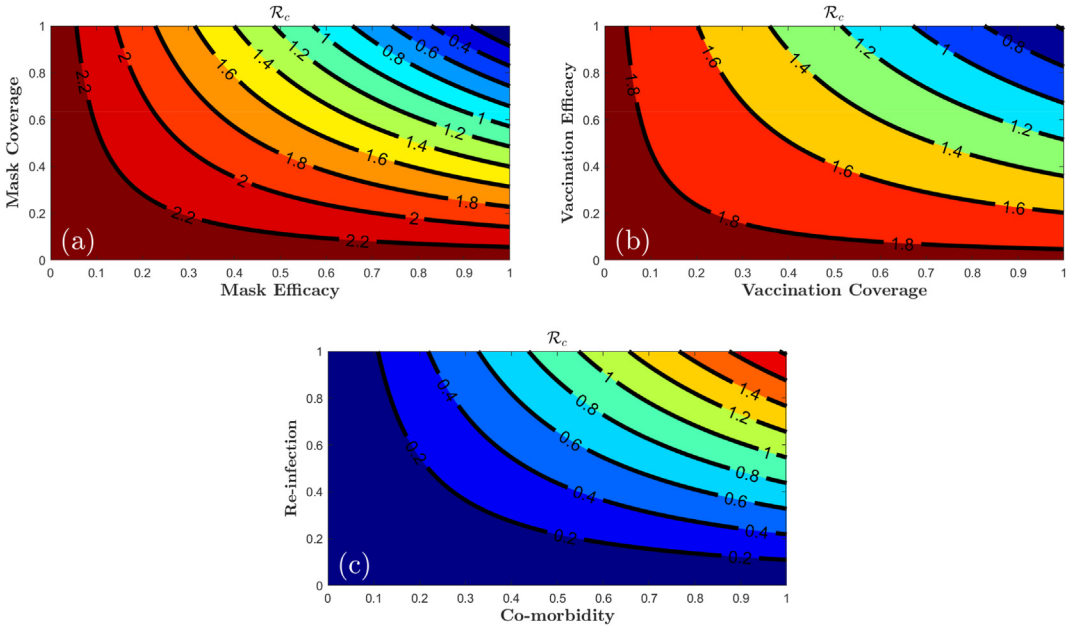

Fig. 12. Fig. 12 (a) Contour plots of the reproduction number ($\mathscr{R}_c$) as a function of mask coverage (m) and face mask efficacy (e). Fig. 12 (b) Contour plots of the reproduction number ($\mathscr{R}_c$) as a function of vaccine coverage and vaccine efficacy. Fig. 12 (c) Contour plots of the reproduction number ($\mathscr{R}_c$) as a function of re-infection and co-morbidity.

(Fig. 12 (a)) says that if 59% or more of the total population wear face mask with efficacy 57% or more, COVID can be eliminated from the community. The combined effect of vaccine coverage and vaccine efficacy on the basic reproduction is also presented (Fig. 12 (b)) by drawing the contour plot of the reproduction number $\mathscr{R}_c$ as a function of vaccine coverage (ξ_s) and vaccine efficacy (ϵ). From this figure (Fig. 12 (b)) it is observed that if 70% or more of the total population is vaccinated with vaccine of efficacy 65% or more, COVID can be eliminated from the community. The combined effect of re-infection and co-morbidity is shown in Fig. 12 (c) by drawing the contour plot of $\mathscr{R}_c$ as a function of re-infection and co-morbidity. This figure illustrates that high re-infection rate and large number of co-morbid susceptible individuals can increase the disease related burden.

6.4. Optimal control

Now, we will present the results obtained by numerical simulations on the model both without control and with control to illustrate the importance of control means. The total optimality system is divided into two parts: state system and adjoint system. The optimality system is solved by an efficient iterative method which is a combination of forward solving of the state system and backward solving of the adjoint system. We design the following control schemes to explore the effect of each control strategy:

6.4.1. Scheme- 1: single control strategies

Strategy A: Prevention of Covid-19 among susceptible ($u_1 \neq 0$)
Strategy B: Implementation of continuous vaccination ($u_2 \neq 0$)
Strategy C: Case detection and quarantine ($u_3 \neq 0$)
Strategy D: Control in treatment ($u_4 \neq 0$)

Fig. 13 depicts the effect of single control strategies considered in this paper as narrated in subsubsection 6.4.1 for all the infected classes and hospitalized class respectively. From this figure it is clear that among the single control strategies, strategy A is the most effective to reduce the corresponding cases in the infected classes and hospitalized class.

6.4.2. Scheme-2: double control strategies

Strategy E: Combination of u_1 & u_2 ($u_1 \neq 0, u_2 \neq 0, u_3 = 0, u_4 = 0$)

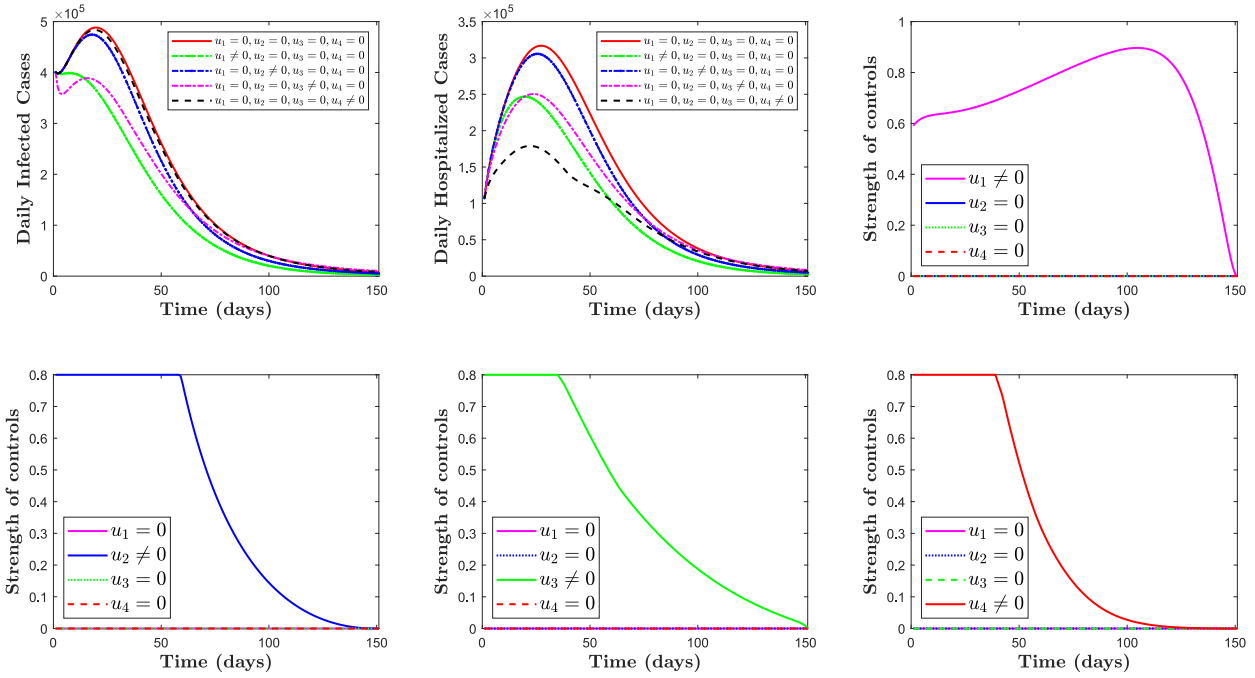

Fig. 13. Dynamics of all infected classes and hospitalized class showing the effect of the optimal strategies in scenario 1.

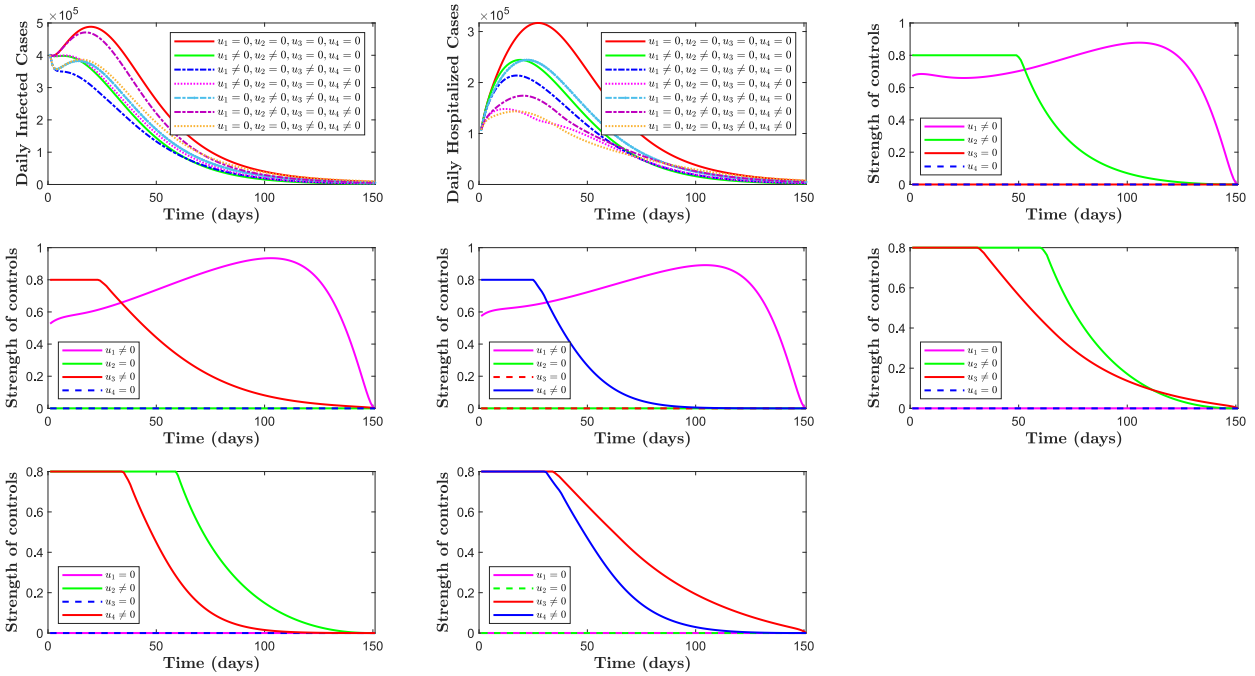

Fig. 14. Dynamics of all infected classes and hospitalized class showing the effect of the optimal strategies in scenario 2.

Strategy F: Combination of u_1 & u_3 ($u_1 \neq 0, u_2 = 0, u_3 \neq 0, u_4 = 0$)
Strategy G: Combination of u_1 & u_4 ($u_1 \neq 0, u_2 = 0, u_3 = 0, u_4 \neq 0$)
Strategy H: Combination of u_2 & u_3 ($u_1 = 0, u_2 \neq 0, u_3 \neq 0, u_4 = 0$)
Strategy I: Combination of u_2 & u_4 ($u_1 = 0, u_2 \neq 0, u_3 = 0, u_4 \neq 0$)
Strategy J: Combination of u_3 & u_4 ($u_1 = 0, u_2 = 0, u_3 \neq 0, u_4 \neq 0$)

Fig. 14 illustrates the comparison among different combination of double control strategies for all the infected classes and hospitalized class respectively as discussed in subsubsection 6.4.2.

6.4.3. Scheme-3: triple control strategies

Strategy K: Combination of u_1, u_2 & u_3 ($u_1 \neq 0, u_2 \neq 0, u_3 \neq 0, u_4 = 0$)
Strategy L: Combination of u_1, u_2 & u_4 ($u_1 \neq 0, u_2 \neq 0, u_3 = 0, u_4 \neq 0$)
Strategy M: Combination of u_1, u_3 & u_4 ($u_1 \neq 0, u_2 = 0, u_3 \neq 0, u_4 \neq 0$)
Strategy N: Combination of u_2, u_3 & u_4 ($u_1 = 0, u_2 \neq 0, u_3 \neq 0, u_4 \neq 0$)

Fig. 15 presents the dynamic of COVID-19 in the presence of various triple control strategies as summarized in subsubsection 6.4.3 for all the infected classes and hospitalized class respectively. From this figure we see that strategy L Scheme 3 of has the lowest number of cases in all the classes. So, strategy L is the most important triple control strategies to reduce the number of cases.

6.4.4. Scheme-4: quadruple control strategy

Strategy O: Combination of u_1, u_2, u_3 & u_4 ($u_1 \neq 0, u_2 \neq 0, u_3 \neq 0, u_4 \neq 0$)

Fig. 16 illustrates the comparison between no control and all the control variables considered at a time for all the infected classes and hospitalized class respectively as described in subsubsection 6.4.4.

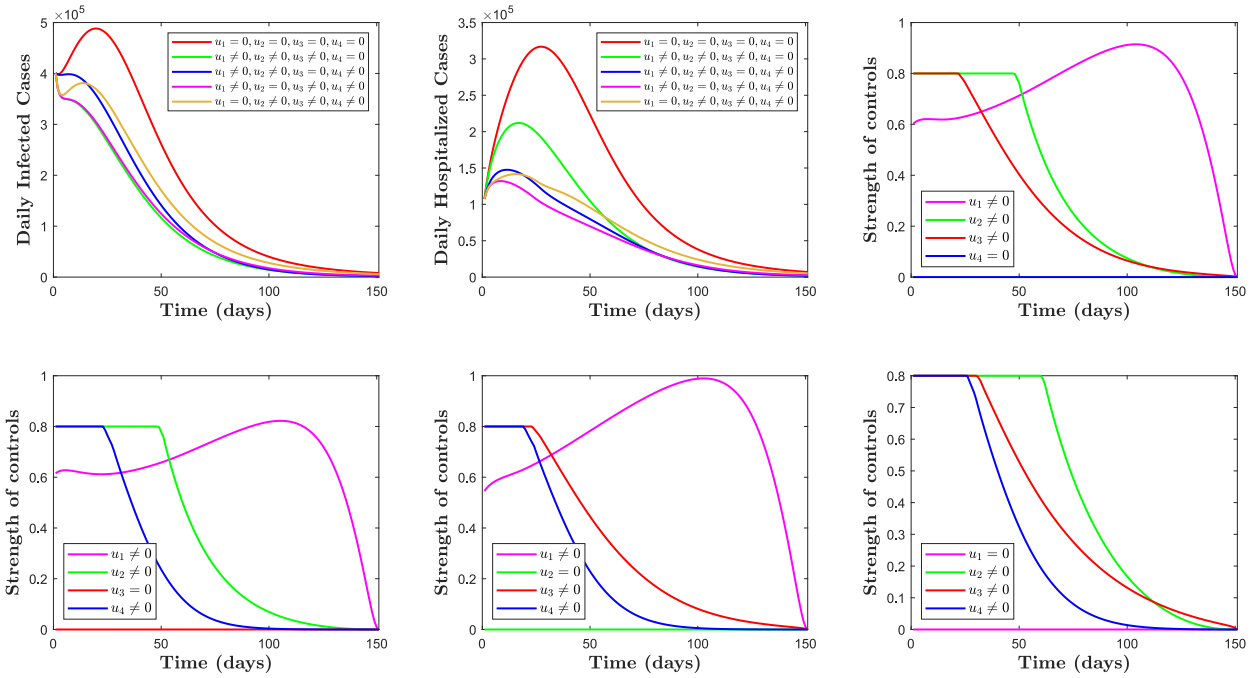

Fig. 15. Dynamics of all infected classes and hospitalized class showing the effect of the optimal strategies in scenario 3.

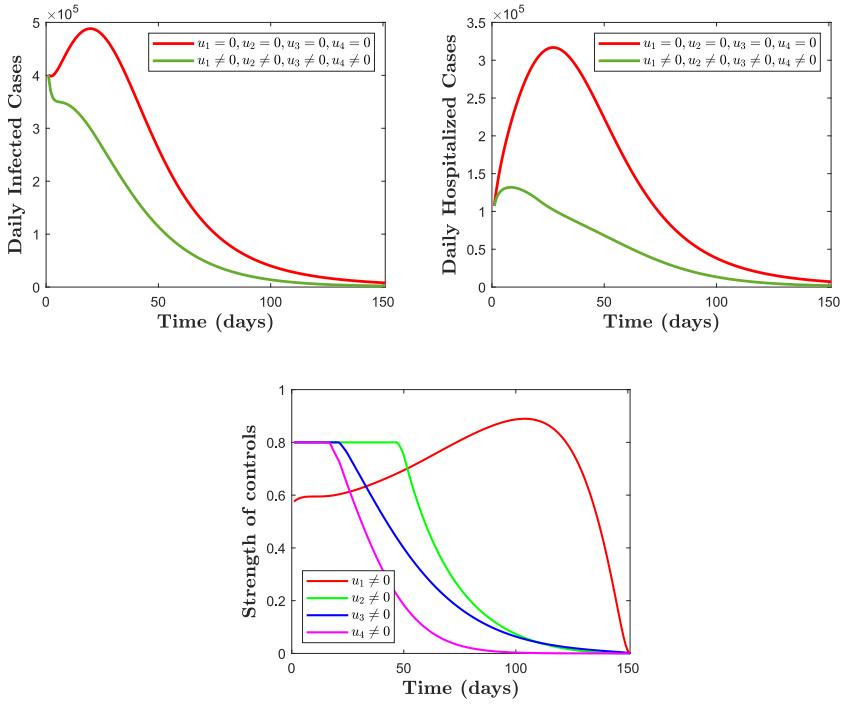

Fig. 16. Dynamical trajectories of all infected classes and hospitalized class showing the effect of the optimal strategies in scenario 4.

7. Conclusion

Since its emergence, COVID-19 has spread rapidly throughout the world posing challenges to the economy and global health. In the beginning, the use of non-pharmaceutical interventions (such as wearing masks publicly, maintaining social

distance, contact tracing, and washing hands) was the only way to control the spread of COVID-19 and to mitigate the disease burden. Now there are numerous vaccines that are proved to be safe and effective against some specific strains, but the frequent appearance of new variants due to the change of virus genetic pattern makes it ineffective against the variants of concern. In this situation, vaccines only will not be able to eliminate the COVID-19 pandemic. So, a combination of mass vaccination program with the implementation of NPIs will be the most effective way to reduce the disease burden. To address these situations and to assess the impact of vaccination, NPIs and other optimal control strategies on the dynamical behavior of COVID-19, a mathematical model is developed and analyzed. We started with some theoretical analysis of the model. We discussed about the positivity and boundedness of the model solutions and it was shown that all the solutions of state variables are positive and bounded. After that, we calculated the basic reproduction number ($\mathscr{R}_c$). It was shown that the disease free equilibrium is locally asymptotically stable whenever $\mathscr{R}_c < 1$. The model is shown to have backward bifurcation where a stable DFE co-exists with a stable EEP when $\mathscr{R}_c < 1$. Then we performed theoretical analysis for the case when there is no re-infection. The disease free equilibrium point (DFE) of model with no re-infection ($\alpha = 0$) is globally asymptotically stable whenever $\mathscr{R}_c < 1$. The unique endemic equilibrium point (EEP) of model with no re-infection is globally asymptotically stable when $\mathscr{R}_c > 1$. Then we analyzed the model numerically. We performed global sensitivity and uncertainty analysis to determine the most influential parameters those controls the dynamics of COVID-19. PRCC analysis suggests that mask coverage (m), mask efficacy (e), effective contact rate (β), vaccine coverage (ξ_s), vaccine efficacy (ϵ) and modification parameter (τ_3) are the top ranked parameters. Numerical simulation of the model suggests that if strict social distance is maintained with the isolation of detected individuals, number of daily infected cases, daily hospitalized cases and cumulative deaths decreases. As for example, Fig. 8 shows that if mild social distancing is followed, the peak of daily infected cases can be reduced by 48%. Further a 74% decrease in the peak of daily infected cases is observed when moderate social distancing is continued. Again if the usage of highly efficacious masks for the maximum number of people can be ensured, the disease burden can be reduced. Fig. 9 (a)–(b) depict that when 25% of total population uses face mask of 25% efficacy, peak value of daily infected cases becomes 365698. But when 50% of total population uses face mask of same efficacy a 16% reduction in the peak value is noticed. Again when 50% of total population uses face mask of 50% efficacy a 49% reduction in the peak value is observed. Numerical result also suggests that a highly effective vaccine with mass vaccine coverage can reduce the prevalence of COVID-19 spread. From Fig. 11 (a) it is evident that when vaccine efficacy increases from 60% to 70%, the peak of the daily infected cases decreases by 23%. Using contour plot (Fig. 12 (a)–(c)), we have shown the combined effect of mask coverage and mask efficacy, vaccine coverage and vaccine efficacy and co-morbidity and re-infection, respectively. Thus if we can isolate the co-morbid susceptible individuals, disease related complexity can be reduced. It is also evident that the presence of re-infection increases the disease burden. Then numerical simulation is carried out for the optimal control problem. In the introduction section, we have discussed the major findings about the optimal control analysis of some related papers. In this paper, control profile of control measure u_1 shows that strategy u_1 rises continuously, reaches to the peak in about 110 days and then drops to zero. Control profile of the second control measure u_2 suggests that this control measure should be maintained at the maximum level for the first 56 days and then gradually reduced to zero. The third control measure (u_3) also needs to be maintained at the maximum level for the first 40 days and then gradually reduced to zero. Control measure u_4 was initially at the maximum level for 18 days and then started to decrease gradually. In Omame et al. (2020), authors showed that among the three control strategies used in their study, the strategy of avoiding COVID-19 infection by co-morbid susceptibles is the most effective one. Study Das et al. (2021) presented that a combination of non-pharmaceutical interventions and vaccination can reduce COVID-19 largely. Again study Shen et al. (2021) suggested a combination of four control strategies (control for isolation, vaccination control, control for rapid testing and identifying infected individuals and treatment control) to reduce COVID-19 infection. In their work Abioye et al. (2021), using three control strategies (control for usage of NPIs, control for active screening with testing and control against reinfection) authors recommended that multifaceted approach is required to fight against COVID-19. Optimal control analysis in Bandekar and Ghosh (2022) reveals that if policies related to testing, contact tracing, and mask-wearing are implemented, the spread of COVID-19 can be reduced. Implementing four control strategies and considering all possible combinations of the strategies, authors in Asamoah et al. (2022) proposed that practicing physical or social distancing protocols is the most cost-effective strategy. Optimal control analysis of our study shows that control strategy considering all the four control variables at a time (Strategy-O) averts the maximum number of COVID-19 cases. But our study suggests that control that ensures continuous vaccination (control measure u_2, strategy-B) is the most cost-effective control strategy to avert the daily infected cases which is a novel finding of this paper.In summary, this study indicates that using an effective vaccine with NPIs, particularly reducing contact rate and increasing quarantined of confirmed cases can eliminate COVID-19. The study also suggests that increasing awareness among general people towards preventing COVID-19 infection is the most effective control strategy to reduce the prevalence of COVID-19. It also reveals that in the presence of re-infection and co-morbidity COVID related complexity can increase.

Declaration of competing interest

The authors declare that they have no known competing financial interests or personal relationships that could have appeared to influence the work reported in this paper.

References

Abioye, A. I., Peter, O. J., Ogunseye, H. A., Oguntolu, F. A., Oshinubi, K., Ibrahim, A. A., & Khan, I. (2021). Mathematical model of covid-19 in Nigeria with optimal control. *Results in Physics, 28*, Article 104598.

Alemneh, H. T., & Alemu, N. Y. (2021). Mathematical modeling with optimal control analysis of social media addiction. *Infectious Disease Modelling, 6*, 405–419.

Asamoah, J. K. K., Okyere, E., Abidemi, A., Moore, S. E., Sun, G.-Q., Jin, Z., Acheampong, E., & Gordon, J. F. (2022). Optimal control and comprehensive cost-effectiveness analysis for covid-19. *Results in Physics, 33*, Article 105177.

Atangana, A. (2020). Modelling the spread of covid-19 with new fractal-fractional operators: Can the lockdown save mankind before vaccination? *Chaos, Solitons & Fractals, 136*, Article 109860.

Bandekar, S. R., & Ghosh, M. (2022). Mathematical modeling of covid-19 in India and its states with optimal control. *Modeling Earth Systems and Environment, 8*(2), 2019–2034.

Blower, S. M., & Dowlatabadi, H. (1994). *Sensitivity and uncertainty analysis of complex models of disease transmission: An hiv model, as an example*. International Statistical Review/Revue Internationale de Statistique.

Boyce, W. E., & DiPrima, R. C. (2020). *Elementary differential equations and boundary value problems*. Wiley.

Bubar, K. M., Reinholt, K., Kissler, S. M., Lipsitch, M., Cobey, S., Grad, Y. H., & Larremore, D. B. (2021). Model-informed covid-19 vaccine prioritization strategies by age and serostatus. *Science, 371*(6532), 916–921.

Carr, J. (2012). *Applications of centre manifold theory, ume 35*. Springer Science & Business Media.

Castillo-Chavez, C., & Song, B. (2004). Dynamical models of tuberculosis and their applications. *Mathematical Biosciences and Engineering, 1*(2), 361.

Center for disease control and prevention. Coronavirus disease 2019 safety-of-vaccines. https://www.cdc.gov/coronavirus/2019-ncov/vaccines/safety/safety-of-vaccines.html. (Accessed 15 May 2022).

Center for disease control and prevention, coronavirus disease. 2019 fully-vaccinated, 15 May 2022 https://www.cdc.gov/coronavirus/2019-ncov/vaccines/fully-vaccinated.html.

Chavez, C. C., Feng, Z., & Huang, W. (2002). On the computation of r0 and its role on global stability. *Mathematical Approaches for Emerging and Re-emerging Infection Diseases: An Introduction, 125*, 31–65.

Das, P., Upadhyay, R. K., Misra, A. K., Rihan, F. A., Das, P., & Ghosh, D. (2021). Mathematical model of covid-19 with comorbidity and controlling using non-pharmaceutical interventions and vaccination. *Nonlinear Dynamics, 106*(2), 1213–1227.

Diekmann, O., Heesterbeek, J. A. P., & Metz, J. A. (1990). On the definition and the computation of the basic reproduction ratio r 0 in models for infectious diseases in heterogeneous populations. *Journal of Mathematical Biology, 28*(4), 365–382.

Ferguson, N. M., Laydon, D., Nedjati-Gilani, G., Imai, N., Ainslie, K., Baguelin, M., Bhatia, S., Boonyasiri, A., Cucunubá, Z., Cuomo-Dannenburg, G., et al. (2020). *Impact of non-pharmaceutical interventions (npis) to reduce covid-19 mortality and healthcare demand. imperial college covid-19 response team*. Imperial College COVID-19 Response Team.

Fleming, W. H., & Rishel, R. W. (2012). *Deterministic and stochastic optimal control, ume 1*. Springer Science & Business Media.

Gumel, A. B., Iboi, E. A., Ngonghala, C. N., & Ngwa, G. A. (2021). *Mathematical assessment of the roles of vaccination and non-pharmaceutical interventions on covid-19 dynamics: A multigroup modeling approach*. medRxiv, 2020–12.

Hethcote, H. W. (2000). The mathematics of infectious diseases. *SIAM Review, 42*(4), 599–653.

Ivorra, B., Ferrández, M. R., Vela-Pérez, M., & Ramos, A. M. (2020). Mathematical modeling of the spread of the coronavirus disease 2019 (covid-19) taking into account the undetected infections. the case of China. *Communications in Nonlinear Science and Numerical Simulation, 88*, Article 105303.

Jain, V., & Yuan, J.-M. (2020). Predictive symptoms and comorbidities for severe covid-19 and intensive care unit admission: A systematic review and meta-analysis. *International Journal of Public Health, 65*(5), 533–546.

Khan, M. A., & Atangana, A. (2020). Modeling the dynamics of novel coronavirus (2019-ncov) with fractional derivative. *Alexandria Engineering Journal, 59*(4), 2379–2389.

Kim, S., Aurelio, A., & Jung, E. (2018). Mathematical model and intervention strategies for mitigating tuberculosis in the Philippines. *Journal of Theoretical Biology, 443*, 100–112.

Kucharski, A. J., Russell, T. W., Diamond, C., Liu, Y., Edmunds, J., Funk, S., Eggo, R. M., Sun, F., Jit, M., Munday, J. D., et al. (2020). Early dynamics of transmission and control of covid-19: A mathematical modelling study. *The Lancet Infectious Diseases, 20*(5), 553–558.

Lakshmikantham, V., Leela, S., & Martynyuk, A. A. (1989). *Stability analysis of nonlinear systems*. Springer.

LaSalle, J. P. (1976). *The stability of dynamical systems*. SIAM.

Le, T. T., Cramer, J. P., Chen, R., & Mayhew, S. (2020). Evolution of the covid-19 vaccine development landscape. *Nature Reviews Drug Discovery, 19*(10), 667–668.

Li, T., & Guo, Y. (2022). Modeling and optimal control of mutated covid-19 (delta strain) with imperfect vaccination. *Chaos, Solitons & Fractals, 156*, Article 111825.

Majumder, M., Tiwari, P. K., & Pal, S. (2022). Impact of saturated treatments on hiv-tb dual epidemic as a consequence of covid-19: Optimal control with awareness and treatment. *Nonlinear Dynamics*, 1–34.

Mancuso, M., Eikenberry, S. E., & Gumel, A. B. (2021). Will vaccine-derived protective immunity curtail covid-19 variants in the us? *Infectious Disease Modelling, 6*, 1110–1134.

Marino, S., Hogue, I. B., Ray, C. J., & Kirschner, D. E. (2008). A methodology for performing global uncertainty and sensitivity analysis in systems biology. *Journal of Theoretical Biology, 254*(1), 178–196.

Mizumoto, K., & Chowell, G. (2020). Transmission potential of the novel coronavirus (covid-19) onboard the diamond princess cruises ship, 2020. *Infectious Disease Modelling, 5*, 264–270.

Ndii, M. Z., & Adi, Y. A. (2021). Understanding the effects of individual awareness and vector controls on malaria transmission dynamics using multiple optimal control. *Chaos, Solitons & Fractals, 153*, Article 111476.

Ngonghala, C. N., Iboi, E., Eikenberry, S., Scotch, M., MacIntyre, C. R., Bonds, M. H., & Gumel, A. B. (2020). Mathematical assessment of the impact of non-pharmaceutical interventions on curtailing the 2019 novel coronavirus. *Mathematical Biosciences, 325*, Article 108364.

Okuonghae, D., & Omame, A. (2020). Analysis of a mathematical model for covid-19 population dynamics in lagos, Nigeria. *Chaos, Solitons & Fractals, 139*, Article 110032.

Omame, A., Sene, N., Nometa, I., Nwakanma, C. I., Nwafor, E. U., Iheonu, N. O., & Okuonghae, D. (2020). Analysis of covid-19 and comorbidity co-infection model with optimal control. *Optimal Control Applications and Methods, 42*, 1568–1590.

Pontryagin, L. S. (1987). *Mathematical theory of optimal processes*. CRC press.

Saha, A. K., Podder, C. N., & Niger, A. M. (2022). Dynamics of novel covid-19 in the presence of co-morbidity. *Infectious Disease Modelling, 7*, 138–160.

Shen, Z.-H., Chu, Y.-M., Khan, M. A., Muhammad, S., Al-Hartomy, O. A., & Higazy, M. (2021). Mathematical modeling and optimal control of the covid-19 dynamics. *Results in Physics, 31*, Article 105028.

Shuai, Z., & Driessche, P. D. (2013). Global stability of infectious disease models using lypunov functions. *SIAM Journal on Applied Mathematics, 73*(4), 1513–1532.

Srivastav, A. K., Tiwari, P. K., Srivastava, P. K., Ghosh, M., & Kang, Y. (2021). A mathematical model for the impacts of face mask, hospitalization and quarantine on the dynamics of covid-19 in India: Deterministic vs. stochastic. *Mathematical Biosciences and Engineering, 18*(1), 182–213.

Taylor, R. (1990). Interpretation of the correlation coefficient: A basic review. *Journal of Diagnostic Medical Sonography, 6*(1), 35–39.

Van den Driessche, P., & Watmough, J. (2002). Reproduction numbers and sub-threshold endemic equilibria for compartmental models of disease transmission. *Mathematical Biosciences, 180*(1–2), 29–48.

World health organization. emergencies, novel corona virus, disease outbreak. https://www.who.int/emergencies/diseases/novel-coronavirus-2019. (Accessed 20 April 2022).
World health organization, emergencies, preparedness, response. Pneumonia of unknown origin – China. https://www.who.int/csr/don/05-january-2020-pneumonia-of-unkown-cause-china/en/. (Accessed 15 May 2022).
Worldometers. (2019). Coronavirus disease. https://www.worldometers.info/coronavirus/country/us. (Accessed 20 April 2022).
World health organization timeline – covid-19. news-room, questions-and-answers. https://www.who.int/news-room/questions-and-answers/item/coronavirus-disease-(covid-19)-vaccines. (Accessed 15 May 2022).
World health organization timeline – covid-19. World health organization (who). 27 april 2020. archived from the original on 29 april 2020. retrieved 2 may 2020 https://www.who.int/emergencies/diseases/novel-coronavirus-2019. (Accessed 15 May 2022).
Wu, J. T., Leung, K., & Leung, G. M. (2020). Nowcasting and forecasting the potential domestic and international spread of the 2019-ncov outbreak originating in wuhan, China: A modelling study. *The Lancet, 395*(10225), 689–697.
Zamir, M., Abdeljawad, T., Nadeem, F., Wahid, A., & Yousef, A. (2021). An optimal control analysis of a covid-19 model. *Alexandria Engineering Journal, 60*(3), 2875–2884.